Frequency moments of cubic metals and substitutional impurities: A critical review of impurity-host force-constant changes from Mössbauer data*

J. M. Grow,† D. G. Howard, R. H. Nussbaum, and M. Takeo
Portland State University, Portland, Oregon 97207
(Received 24 September 1976; revised manuscript received 7 July 1977)

A critical review is presented of various simplified impurity lattice models which have been used in the literature to extract effective host-impurity force-constant ratios from Mössbauer fraction and thermal-shift measurements in highly dilute alloys. It is shown that the use of some popular models, sometimes in combination with inappropriately matched dynamical parameters of the host, has led to a systematic underestimate of the range of force-constant changes for ^{57}Fe, ^{119}Sn, and ^{197}Au impurity systems. Mannheim's analytical impurity model provides at present the most practical and physically meaningful theoretical framework for an internally consistent method of analysis of Mössbauer lattice-dynamics experiments in cubic metals. A new and useful set of analytical relationships has been derived from the Mannheim model, expressing experimentally obtainable impurity to host moment ratios in terms of mass and force-constant ratios. Moments and their ratios have been calculated for some theoretical lattice models and 18 cubic metals and rare-gas solids for which neutron dispersion data are available. A uniform general force Born–von Kárman model was used in combination with elastic constants to assure internal consistency among the resulting data. Moment analyses of heat-capacity data for most metals used as hosts for impurity studies were performed in parallel. Generally, we found good agreement between these two independent sets of results. Remarkable uniformity and trends were found within the groups of fcc and bcc metals for the values of certain moment ratios. A summary of most reliable Mössbauer f data for ^{57}Fe, ^{119}Sn, and ^{197}Au is presented, including some new experimental results for ^{57}Fe in Ir, Nb, and Rh. Using these impurity data in combination with the host data presented leads to a set of internally consistent effective host-impurity force-constant ratios which span a range $0.65 < A/A' < 2.6$ for a range of mass ratios $0.3 < M'/M < 3.5$. Several of the new values differ considerably from those in the literature. This study shows that no single host parameter is well correlated with the observed changes in force-constant ratio for a given impurity, despite earlier suggestions to the contrary. The observed trends must, therefore, depend upon a combination of several host parameters as yet not understood.

I. INTRODUCTION

A. Inconsistencies in the literature

One of the parameters which has been studied in various dilute alloy experiments is the ratio of the effective host-host to impurity-host interaction (the effective host-impurity force constant ratio) resulting from the substitution of isolated impurity atoms for host atoms in various metals. In particular, a great number of studies of the Mössbauer effect of impurity atoms in metal hosts, measuring recoil-free fractions and thermal shifts, have been analyzed with the help of various impurity lattice models to estimate such effective interatomic force constant changes and to search for trends. Some earlier systematic studies[1-3] concluded that impurity-host force constants for Fe and Sn impurities do not, in general, differ significantly from host-host force constants. These results were derived from methods of data analysis which tend to reduce the apparent force-constant changes by a combination of several factors: (i) impurity data with rather large experimental errors, (ii) inappropriately chosen parameters to represent the host lattice properties, and (iii) the use of oversimplified theoretical models. While only the first of these three factors is included in stated error bars, the other two factors introduced equally large or larger systematic errors and ambiguities into the interpretation of such results. Some recent studies, using more reliable experimental data for both the solid solution and the pure host metals, and a more sophisticated theoretical analysis,[4,5] yielded effective host-impurity force constant ratios in a variety of cubic hosts which deviate quite significantly from the predictions of an isotopic impurity model (mass change without changes in force constants).

Our aim in this paper is to critically review the major methods of data analysis hitherto used in such studies, to point out some of the unnecessary oversimplifications which have caused relatively large systematic errors to be propagated through the literature in this field, and to suggest an internally consistent and physically less ambiguous methodology for the lattice-dynamical analysis of Mössbauer experiments involving substitutional impurities.

B. Organization of this paper

In Sec. II we review definitions of *pure lattice* (host) *moments*, *impurity site moments*, and use-

ful *effective force constants*. We follow this with a review of the most commonly cited impurity models and those explicit and implicit approximations which are responsible for systematic errors. We then propose an alternative method of analysis, applicable to quasiharmonic cubic systems, based on Mannheim's impurity model[6] and using experimentally determined impurity and host frequency moments.

In Sec. III we present some new analytical results derived from Mannheim's theory, expressing impurity site to host moment ratios as simple functions of mass and force-constant ratios, respectively. These relations are exact within the assumptions of the model for the even moments (see Appendix). Corresponding approximate relations for some useful odd moments were obtained from a numerical analysis, applying the same impurity theory[6] to a limited range of mass and force-constant changes.

In Sec. IV we discuss certain regularities in moment ratios among face-centered-cubic (fcc) and body-centered-cubic (bcc) pure metals and noble-gas solids. These data were derived from a uniform Born–von Kármán analysis of neutron dispersion experiments, combined with elastic constants. We also compare these frequency moments with those we have obtained independently from heat-capacity data. The observed regularities and trends in host moment ratios could, in turn, be used to estimate moment ratios in similar pure metals for which no complete set of moments is available.

In Sec. V we summarize the best available Mössbauer f values, including some new data, for Fe, Sn, and Au impurities in cubic metals, from which we obtained a set of internally consistent effective nearest-neighbor host-impurity force constant ratios. They were calculated by combining the impurity f data with the analytical results of the impurity theory (Sec. III) and the host metal properties (Sec. IV).

In Sec. VI we discuss the limitations of the possible use of Mössbauer thermal-shift measurements as an independent means for obtaining effective impurity-host force constant ratios with a precision comparable to that obtainable by f measurements. In particular, we will show that an earlier reported empirical linear relation between f and shift data is to be expected from our theoretical analysis. On the other hand, a reportedly unexpected empirical correlation between a ratio of impurity-site moments at high and low temperatures and the host Debye temperatures, modified by the host to impurity mass ratio, is found to be substantially weakened by inclusion of all of the most reliable available data. Another proposed correlation between the effective impurity-host force-constant ratio and a nearest-neighbor bond-stretching force constant of the host material is similarly weakened by the complete set of available data.

However, for ^{57}Fe impurities only, there seems to exist a *qualitative* correlation between an increased effective impurity-to-host force constant (compared to the host-host interaction) and an increase in lattice parameter upon alloying Fe with the host metal.

We conclude, based on all presently available reliable data, that no one single host parameter is simply correlated with the variations in effective host-impurity force-constant ratios from material to material.

II. HOST MOMENTS, IMPURITY MOMENTS, AND EFFECTIVE FORCE CONSTANTS IN CUBIC SOLID SOLUTIONS

A. Relation of impurity-site moments to Mössbauer fraction and thermal-shift measurements

It is well known that the measurable absolute value of the Mössbauer fraction $f(T)=\exp(-\kappa^2\langle x^2\rangle_T)$ (κ is the γ-ray wave number and $\langle x^2\rangle_T$ is the mean-squared displacement of the radiating atom) and the thermal or second-order Doppler shift (SOD) $\Delta E/E=\langle v^2\rangle_T/(2c^2)$ for an isolated impurity atom in a pure and quasiharmonic lattice at high and at low temperatures are directly related to certain moments of the impurity dynamic-response function. We refer to the thorough analysis by Housley and Hess[7] for discussion and references. This work is an extension of theirs, applying it to Mannheim's impurity theory.[6]

At high temperatures ($T \gtrsim \frac{1}{2}\Theta_D$),

$$\langle x^2\rangle_T^{\mathrm{imp}} = \frac{kT}{M'}\left[\mu'(-2)+\frac{1}{12}\left(\frac{\hbar}{kT}\right)^2 - \frac{1}{720}\left(\frac{\hbar}{kT}\right)^4\mu'(2)+\cdots\right], \tag{1a}$$

$$\langle v^2\rangle_T^{\mathrm{imp}} = \frac{3kT}{M'}\left[1+\frac{1}{12}\left(\frac{\hbar}{kT}\right)^2\mu'(2) - \frac{1}{720}\left(\frac{\hbar}{kT}\right)^4\mu'(4)+\cdots\right], \tag{1b}$$

and at $T\to 0$ (in practice, near liquid-He temperature[7]),

$$\langle x^2\rangle_0^{\mathrm{imp}} = (\hbar/2M')\mu'(-1), \tag{1c}$$

$$\langle v^2\rangle_0^{\mathrm{imp}} = (3\hbar/2M')\mu'(1). \tag{1d}$$

In the above equations k is Boltzmann's constant and M' is the mass of the impurity atom. The quantities $\mu'(n)$ are impurity-site moments which have been defined in the Appendix.

B. Definitions of lattice-dynamical parameters

The dynamical properties of a monatomic lattice in the harmonic approximation can generally be calculated if the distribution of the quantized normal modes of vibration is known. These are usually given in terms of a normalized phonon density-of-states function $G(\omega)$. The dynamical quantities themselves can then be expressed as statistically weighted integrals over all frequencies. In the limiting cases of high or low temperatures, the statistical factor of the integrand can be expanded into a suitable power series so that the resulting integrals are weighted averages of particular powers of the frequency[7]: the *moments* of the phonon density of states function

$$\mu(n)=\int_0^\infty \omega^n G(\omega)\,d\omega, \quad \mu(0)=1. \tag{2a}$$

Similarly, when we consider an isolated substitutional *impurity*, its response to the phonons of the host lattice is given by the dynamic response function[4,6] $G'(\omega)$ (see Sec. III A), and the motion of the impurity at high and low temperatures is governed by a similar expansion involving the corresponding impurity site moments[7] [see Appendix equations (A11), (A12), and (A13)]

$$\mu'(n)=\int_0^\infty \omega^n G'(\omega)\,d\omega, \quad \mu'(0)=1. \tag{2b}$$

Alternatively, these moments, Eqs. (2a) and (2b), can be used instead of the distribution functions for describing the dynamical properties of the host or the impurity. In particular, it has been shown[7] that for any harmonic monatomic cubic crystal with central or noncentral all-neighbor interactions

$$\mu(+2)=A_{xx}(0,0)/M, \tag{3a}$$

with

$$A_{xx}(0,0)=-\sum_{l\neq 0} A_{xx}(0,l), \tag{3b}$$

where $A_{xx}(0,l)$ are second derivatives of a two-body potential,[6] between atoms at the origin and at the lattice site l, and M is the mass of an atom of the host. $A_{xx}(0,0)$ represents the restoring force in the x direction per unit displacement in the x direction of an atom at the origin[7] (all other atoms being held fixed at their equilibrium positions l). For a substitutional impurity atom at the origin, we can define $A'_{xx}(0,0)$ in an analogous way as the *restoring force* in the x direction per unit displacement in the x direction of the impurity atom at the origin (holding all other atoms fixed at their equilibrium positions). The (+2)-impurity-site moment is directly related to the impurity restoring force and the impurity mass M'[7]

$$A'_{xx}(0,0)=-\sum_{l\neq 0} A'_{xx}(0,l) \tag{3c}$$

and

$$\mu'(+2)=A'_{xx}(0,0)/M'. \tag{3d}$$

Because of their unambiguous and model-independent physical meaning, we will consider in this paper the host or impurity *restoring force constants* $A_{xx}(0,0)\equiv A$ and $A'_{xx}(0,0)\equiv A'$ as the effective force constants [see Eq. (12) in Ref. 7].

For a pure material $\mu(+2)$ (and thus A) can be determined directly from an appropriate phonon-distribution function $G(\omega)$, based, e.g., on neutron-dispersion data. We have calculated $G(\omega)$ for all the cubic materials listed in Table I, using a general force Born–von Kármán model fit to precision neutron-dispersion data (see Sec. IV A). Therefore, the restoring forces A for all host materials discussed in this study contain contributions up to sixth or seventh nearest neighbors [see Eqs. (3a) and (3b)]. In fcc metals the first-nearest-neighbor central-force term is generally (within a few percent) equal to the overall restoring force A. This is due to alternating signs producing cancellations in the total sums. Alternatively, A can also be obtained from $\mu(+2)$ derived from heat capacities (see Sec. IV B).

On the other hand, in order to obtain analytical relations of host-to-impurity moment ratios as functions of force constant and mass ratios (see Appendix), we had to restrict ourselves to the *central-force nearest-neighbors approximation* (nn) of Mannheim's model[6]: $A=-\sum_{l\neq 0}^{nn} A_{xx}(0,l)$ and $A'=-\sum_{l\neq 0}^{nn} A'_{xx}(0,l)$. The force constant ratio A/A' appearing in those analytical relations, when used in conjunction with an experimentally determined (and unrestricted) value of A, can thus be interpreted as a ratio of *effective nearest-neighbor host-to-impurity restoring forces*. For brevity's sake, we will call this ratio the *effective host-impurity force-constant ratio* A/A'.

It should be noted that in general, A, A', and A/A' must be considered as temperature dependent[8] due to anharmonic effects. Consequently, $G(\omega)$, $G'(\omega)$, and their moments are, in general, also functions of temperature. For example, in copper A and $\mu(-2)$ change by about 2% per 100 K.[8]

Because of the model-independent relation of $\mu(+2)$ to the host-restoring force A [Eq. (3a)], it is convenient to relate the other moments of the host-phonon distribution function $G(\omega)$ to $\mu(+2)$ by defining the dimensionless ratios

$$\beta_n=[\mu(+2)]^{n/2}/\mu(n). \tag{4}$$

TABLE I. Moment ratios and elastic constants for a number of cubic lattice models and cubic metals. (Details of the models are discussed in Sec. IV.)

Lattice	Models T (K)	Ref.	Cutoff frequencies (10^{26} rad^2/sec^2) $A/M=\mu(+2)$	$\frac{1}{2}\omega^2_{max}$	Moment ratios β_{-2}	β_{-1}	β_{+1}	β_{+4}	Elastic constants (10^{12} dyn/cm^2) C_{11}	C_{12}	C_{44}	Ref.
Einstein	···	···	···	···	1.0	1.0	1.0	1.0	···	···	···	···
Debye	···	···	···	···	0.556	0.861	1.033	0.840	···	···	···	···
Visscher	···	a	···	···	0.660	0.897	1.026	0.857	···	···	···	···
Leighton	···	b	···	···	0.596	0.865	1.037	0.800	···	···	···	···
fcc:												
Al	80	c	16.91	18.73	0.556	0.842	1.046	0.759	1.137	0.619	0.313	t
Ni	RT	d	15.29	15.54	0.603	0.865	1.038	0.797	2.508	1.500	1.235	u
Cu	RT	e	10.10	10.79	0.559	0.848	1.042	0.779	1.684	1.214	0.754	u
Kr	10	f	0.44	0.45	0.555	0.851	1.041	0.782	0.0514	0.0284	0.0268	f
Pd	RT	e	8.30	9.46	0.509	0.830	1.046	0.765	2.271	1.761	0.717	u
Ag	RT	g	4.85	5.22	0.524	0.833	1.047	0.763	1.240	0.937	0.461	u
Xe	10	h	0.33	0.33	0.558	0.852	1.041	0.784	0.0527	0.0282	0.0295	h
Pt	90	i	5.85	6.75	0.506	0.823	1.050	0.747	3.536	2.510	0.769	v
Au	RT	j	3.45	4.32	0.443	0.788	1.063	0.695	1.923	1.631	0.420	u
Pb	100	k	0.92	1.01	0.491	0.801	1.061	0.702	0.544	0.451	0.182	k
bcc:												
Na	90	l	2.84	2.88	0.454	0.791	1.057	0.747	0.0793	0.0641	0.0596	w
Cr	RT	m	21.90	18.21	0.691	0.910	1.022	0.879	3.500	0.678	1.008	m
Fe	RT	n	18.02	16.99	0.599	0.870	1.034	0.818	2.431	1.381	1.219	x
Rb	120	o	0.40	0.43	0.382	0.753	1.068	0.712	0.0314	0.0264	0.0189	y
Nb	RT	p	8.28	8.51	0.534	0.851	1.037	0.816	2.400	1.260	0.281	z
Mo	RT	q	14.43	13.01	0.674	0.904	1.024	0.865	4.60	1.76	1.10	x
Ta	RT	r	5.24	5.22	0.617	0.880	1.030	0.845	2.609	1.574	0.818	u
W	RT	s	9.83	9.10	0.658	0.894	1.028	0.842	5.233	2.045	1.607	u

[a] Reference 9.
[b] R. B. Leighton, Rev. Mod. Phys. 20, 165 (1948).
[c] G. Gilat and R. M. Nicklow, Phys. Rev. 143, 487 (1966).
[d] R. J. Birgeneau, J. Cordes, G. Dolling, and A. D. B. Woods, Phys. Rev. 136, A1359 (1964).
[e] Reference 17.
[f] J. Skalyo, Jr., Y. Endoh, and G. Shirane, Phys. Rev. B 9, 1797 (1974).
[g] W. A. Kamitakahara and B. N. Brockhouse, Phys. Lett. A 29, 639 (1969).
[h] N. A. Lurie, G. Shirane, and J. Skalyo, Jr., Phys. Rev. B 9, 5300 (1974).
[i] D. H. Dutton, B. N. Brockhouse, and A. P. Miiller, Can. J. Phys. 50, 2915 (1972).
[j] J. W. Lynn, H. G. Smith, and R. M. Nicklow, Phys. Rev. B 8, 3493 (1973).
[k] B. N. Brockhouse, T. Arase, G. Caglioti, K. R. Rao, and A. D. B. Woods, Phys. Rev. 128, 1099 (1962).
[l] A. D. B. Woods, B. N. Brockhouse, R. H. March, and A. T. Stewart, Phys. Rev. 128, 1112 (1962).
[m] W. M. Shaw and L. D. Muhlestein, Phys. Rev. B 4, 969 (1971).
[n] V. J. Minkiewicz, G. Shirane, and R. Nathans, Phys. Rev. 162, 528 (1967).
[o] J. R. D. Copley and B. N. Brockhouse, Can. J. Phys. 51, 657 (1973).
[p] Y. Nakagawa and A. D. B. Woods, Phys. Rev. Lett. 11, 271 (1963).
[q] A. D. B. Woods and S. H. Chen, Solid State Commun. 2, 233 (1964).
[r] A. D. B. Woods, Phys. Rev. 136, A781 (1964).
[s] S. H. Chen and B. N. Brockhouse, Solid State Commun. 2, 73 (1964).
[t] G. N. Kamm and G. A. Alers, J. Appl. Phys. 35, 327 (1964).
[u] C. Kittel, *Phonons*, edited by R. W. H. Stevenson (Plenum, New York, 1966), p. 14.
[v] R. E. MacFarlane, J. A. Rayne, and C. K. Jones, Physics Lett. 18, 91 (1965).
[w] M. E. Diederich and J. Trivisonno, J. Phys. Chem. Solids 27, 637 (1966).
[x] O. L. Anderson, *Physical Acoustics*, Vol. III, Part B, edited by W. P. Mason (Academic, New York, 1965), p. 77.
[y] E. J. Gutman and J. Trivisonno, J. Phys. Chem. Solids 28, 805 (1967).
[z] P. E. Armstrong, J. M. Dickinson, and H. L. Brown, Trans. Metall. Soc. AIME 236, 1404 (1966); D. I. Bolef, J. Appl. Phys. 32, 100 (1961).

C. Review of some theoretical models commonly used to analyze impurity-host force-constant ratios

1. Einstein model

Many of the analyses of changes in the effective impurity-host force constant in the literature were implicitly based on the *Einstein approximation*. Here, the lattice is treated as a system of independent oscillators, all of frequency $\omega_E=(A/M)^{1/2}$. For this model we have

$$\mu_E(n)=\omega_E^n, \quad \beta_n^E=1 \text{ for all } n. \tag{5}$$

An impurity in the *Einstein model* is thus represented by an altered mass M' with an altered force constant A', which will vibrate at an altered frequency ω_E'. Then

$$\frac{\mu_E'(n)}{\mu_E(n)}=\left(\frac{\omega_E'}{\omega_E}\right)^n=\left(\frac{M}{M'}\right)^{n/2}\left(\frac{A'}{A}\right)^{n/2}. \tag{6}$$

2. Einstein-Debye model

In using an expression such as Eq. (6) to determine the quantity A'/A for a given mass change, one must have data for the moments of both the impurity and the host. For the host, thermodynamic properties, such as heat capacities, have generally been parametrized using the *Debye model*, which assumes a single constant value for the velocity of the phonons, but allows for a range of frequencies up to some maximum value ω_D. For this model and an appropriate normalization condition

$$G_D(\omega)=3\omega^2/\omega_D^3, \quad 0\le\omega\le\omega_D. \tag{7a}$$

Moments and "Debye temperatures" $\Theta_D(n)$ are then defined as

$$\mu_D(n)=\frac{3}{n+3}\,\omega_D^n=\frac{3}{n+3}\left(\frac{k}{\hbar}\right)^n\Theta_D(n)^n, \quad n>-3, \tag{7b}$$

where k is Boltzmann's constant. Here

$$\beta_n^D=\tfrac{1}{3}(n+3)(\tfrac{3}{5})^{n/2}. \tag{7c}$$

It is well known that different dynamical quantities are characterized by different $\Theta_D(n)$ temperatures. Also, different moments $\mu_D(n)$ dominate the low and the high temperature values of these quantities.

For the impurity, traditionally, an "effective Debye temperature" $\Theta_D'(n)$ has been defined from a fit of experimental Mössbauer data to the appropriate Debye function for the particular measured quantity (e.g., $\langle x^2\rangle_T^{\text{imp}}$). Then, using a Debye temperature $\Theta_D(n)$ for the host, the relationship

$$\Theta_D'(n)=\Theta_D(n)(M/M')^{1/2}(\gamma'/\gamma)^{1/2} \tag{7d}$$

defines an effective force-constant ratio γ'/γ. Since Eq. (7d) is based on the *Einstein model*, Eq. (6), γ'/γ represents an Einstein-Debye force-constant ratio. In applying Eq. (7d) to impurity measurements, it is essential for internal consistency that the pure host parameter $\Theta_D(n)$ must represent the same nth Debye moment [Eq. (7b)] which characterizes the measured impurity data, rather than a tabulated average Debye temperature Θ_D. The Einstein-Debye force-constant ratio γ'/γ obtained in this way from Eq. (7d) will only be comparable to our ratio A'/A for those cases where the *Einstein relation*, Eq. (6), can be shown to be approximately valid for a real crystal. We shall show in Sec. III that this is indeed the case for $n=+1$ (low-temperature SOD shift measurements), while for $n=-1$ or -2 (high- and low-temperature mean-squared displacement measurements), the use of Eq. (7d) to obtain impurity-host force-constant changes may introduce rather large errors.

3. Visscher model at low temperature

Some theoretical justification for using Eq. (7d) for real crystals was given by Visscher,[9] based on a simple cubic (sc) lattice model with a single impurity atom, in which the shear and compressional forces were taken to be equal in magnitude. These assumptions lead to dispersion relations in which longitudinal and transverse vibrations have identical frequencies, parametrized by a single variable force constant. Visscher calculated dynamic-response functions based on this model, and analyzed the mean-squared displacement and velocity in the *low-temperature limit* which are determined by $\mu'(-1)$ and $\mu'(+1)$, respectively [see Eqs. (1c) and (1d)]. The results of his computer analysis were given in graphical rather than analytical form. For *small changes in mass and force constants only*, his graphs deviate from the *Einstein model*, Eq. (7d), for $n=-1$ and $+1$, by only a few percent. This is probably the reason why Eq. (7d) is often ascribed to Visscher. However, Visscher's graphs represented only the $T=0$ limit, and it is quite clear that the sc model is rather unphysical. Equation (7d) has nevertheless been used widely to determine Einstein-Debye force constant ratios γ'/γ from impurity mean-squared-displacement measurements at or above room temperature, which are determined by $\mu'(-2)$ rather than by $\mu'(-1)$ [see Eq. (1a)]. We will show in the following sections that the use of the *Einstein-Debye* relation Eq. (7d) in this and other cases may lead to substantial errors.

4. Maradudin-Flinn model at high temperature

Maradudin and Flinn[10] have considered the *high-temperature* behavior of the impurity mean-squared

displacement, which depends upon $\mu'(-2)$ [see Eq. (1a)]. Using as their model an impurity in a face-centered cubic lattice with nearest-neighbor central-force interactions (often referred to as the *Leighton model*), and employing "Ludwig's approximation," they obtain a relation [their Eq. (4.8)] which may be rewritten in the form

$$\left(\frac{\Theta_D(-2)}{\Theta'_D(-2)}\right)^2 = \frac{\mu'(-2)}{\mu(-2)} = \left(\frac{M'}{M}\right) \times\left(1+\frac{(1-A'/A)}{\mu(+2)\mu(-2)} + \frac{5}{4}\,\frac{(1-A'/A)^2}{\mu(+2)\mu(-2)} + \cdots\right). \tag{8}$$

This relation will approximate the Einstein result, Eq. (6), only if the term $\mu(+2)\mu(-2)=1/\beta_{-2}$ is approximately equal to one; for the *Leighton model*, however, $\beta_{-2}=0.596$ (see Table I). Thus we see that the use of the unphysical *Einstein model* may introduce serious errors, even when the appropriately weighted $\Theta_D(-2)$ is used for the host.

While the results of Maradudin and Flinn,[10] Eq. (8), could be used to determine A'/A, the series given in Eq. (8) does not converge except for small changes in force constants, smaller, in fact, than are found for several impurity-host systems (see Sec. V). We will present an alternative to Eq. (8) in Sec. III A which does not suffer from this limitation.

5. *Visscher model at high temperature*

Recently, Ohashi and Kobayashi[11] have extended the Visscher model[9] (Sec. II C 3) to include the *high-temperature limit* for the impurity mean-squared displacement. The result [their Eq. (4.2a)] can be written in terms of the appropriate moments

$$\frac{\mu'(-2)}{\mu(-2)} = \left(\frac{M'}{M}\right)[1-0.675(1-A/A')]. \tag{9}$$

Unlike Eq. (8), this expression is valid for all values of A/A'. It is, however, closely related to Eq. (8), as we shall show in Sec. II C 6. Ohashi and Kobayashi[11] show that for small changes in force constant, Eqs. (8) and (9) agree (see Fig. 5 of their paper); they compare these relations also to Visscher's graphs for $T=0$. This, however, is meaningless since at low temperature $\Theta'_D(n)$ for the impurity mean-squared displacement involves $\mu'_D(-1)$ rather than $\mu'_D(-2)$ [see Eqs. (1a) and (1c)], which explains the difference in slopes in their Fig. 5. Unfortunately, their evaluations of force constant changes from published impurity and host data using Eq. (9) (summarized in their Table I) show gross discrepancies with the values summarized in this work (see Table II); this is in part due to the use of unspecified Debye temperatures Θ_D instead of the appropriately evaluated $\Theta_D(-2)$ values for the host metals.

6. *Mannheim's model for cubic crystals*

Mannheim's theory[6] provides analytical expressions for experimentally important lattice dynamical parameters such as $\langle x^2\rangle_T$ or $\langle v^2\rangle_T$ for an *unrestricted* range of temperature, mass, and effective host-impurity force-constant ratios. To achieve this the following simplifying assumptions had to be made: (i) harmonic impurity-lattice interaction; (ii) only nearest-neighbor central forces are considered (see Sec. II B). Mannheim's theory yields expressions for the dynamical parameters in the form of modified integrals over the presumed to be known phonon density-of-states function $G(\omega)$ for the pure host. The only free parameters are the mass ratio M/M' and the effective force-constant ratio A/A'. Contributions due to the appearance of localized modes are incorporated in the theory. Several aspects of the applications of this theory to the analysis of experimental Mössbauer data will be discussed in greater detail in Secs. II D and III A.

D. Determining effective host-impurity force-constant ratios from Mannheim's impurity model

For cubic impurity systems, Mannheim's theory[6] is the most useful and convenient model available today for the numerical analysis of impurity mean-squared displacements $\langle x^2\rangle_T$ (and/or mean-squared velocities $\langle v^2\rangle_T$) from Mössbauer zero-phonon fraction $f(T)$ (or SOD) measurements. The model predicts the *dynamic-response function* of the impurity atom $G'(\omega)$ for any mass or force-constant change, provided a realistic phonon density-of-states function $G(\omega)$ for the pure host is known. All experimentally accessible dynamical parameters for impurities such as $\langle x^2\rangle_T$ and $\langle v^2\rangle_T$ can be expressed as weighted integrals over the appropriate dynamic response function.[6] We have recently presented arguments[8] that in view of the anharmonic effects in real materials, which cannot be incorporated unambiguously into an analytical impurity theory, we consider the following hierarchy of approximations as optimal in terms of obtaining physically significant *effective host-impurity force-constant ratios* (see Sec. II B) from experimental data.

1. *Extrapolated zero-degree effective host-impurity force-constant ratios*

If phonon density-of-states functions for the pure material are known at high and at low temperatures, measurements of the impurity mean-squared displacement $\langle x^2\rangle_T$ at those same temp-

TABLE II. Effective host-impurity force-constant ratios from Mössbauer data on ^{57}Fe, ^{119}Sn, and ^{197}Au.

			A/A' using neutron dispersion data				A/A' using heat-capacity data	
Impurity	Host	Mass ratio M'/M	From $f(T'), G(\omega)_{T_0}$, and Eq. (10)	Impurity $T'(K)$	Host $T_0(K)$	$\mu'(-1)/\mu(-1)_{\text{disp}}$ $T' \simeq 4$ K; same T_0	$\mu'(-2)/\mu(-2)_{C_p}$ $T' \simeq 296$; $T_0 \simeq 150$ K	$\mu'(-1)/\mu(-1)_{C_p}$ $T' \simeq 4$ K; $T_0 \simeq 150$ K
^{57}Fe	Al	0.47	1.6 ± 0.3	RT	80	···	1.6 ± 0.6	···
	Au	3.46	1.49 ± 0.10	RT	RT	···	1.59 ± 0.08	···
	Cr	0.91	1.43 ± 0.10	RT	RT	···	1.39 ± 0.20	···
	Cu	1.12	*0.76 ± 0.01* [a]	···	···	···	···	···
			0.80 ± 0.10	80	80	0.81 ± 0.13	0.80 ± 0.07	0.80 ± 0.04
			0.82 ± 0.03	RT	RT	···	···	···
			0.87 ± 0.03	471	473	···	···	···
			0.91 ± 0.03	677	673	···	···	···
	Ir	3.38	···	···	···	···	2.15 ± 0.16	2.56 ± 0.40
	Mo	1.69	2.25 ± 0.15	RT	RT	(2.49 ± 0.64)	2.31 ± 0.20	2.55 ± 0.76
	Nb	1.63	1.63 ± 0.09	RT	RT	(2.10 ± 0.50)	1.67 ± 0.10	2.17 ± 0.55
	Ni	1.03	0.80 ± 0.10	RT	RT	···	···	···
	Pd	1.87	*1.72 ± 0.03* [a]	···	···	···	···	···
			1.72 ± 0.02	126	120	1.96 ± 0.50	1.78 ± 0.09	1.94 ± 0.70
			1.78 ± 0.05	RT	RT	···	···	···
			1.71 ± 0.04	655	673	···	···	···
	Pt	3.43	1.60 ± 0.25	78–110	90	1.97 ± 0.40	1.73 ± 0.07	2.16 ± 0.53
	Rh	1.81	···	···	···	···	1.84 ± 0.10	2.32 ± 0.40
	Ta	3.18	1.84 ± 0.08	RT	RT	(2.5 ± 0.7)	1.94 ± 0.15	2.7 ± 0.8
	W	3.23	2.42 ± 0.18	RT	RT	(2.60 ± 1.0)	2.53 ± 0.21	2.9 ± 1.2
^{119}Sn	Ag	0.91	0.98 ± 0.06	RT	RT	(0.97 ± 0.45)	1.11 ± 0.06	1.01 ± 0.40
	Au	1.66	1.02 ± 0.23	RT	RT	(0.53 ± 0.20)	1.26 ± 0.34	0.59 ± 0.20
	Pb	1.74	···	···	RT	(0.40 ± 0.05)	···	···
	Pd	0.89	2.12 ± 0.08 [b]	RT	120	1.78 ± 0.08	2.25 ± 0.06	1.71 ± 0.08
			1.9 ± 0.2 [c]	RT	RT	···	···	···
	Pt	1.64	1.00 ± 0.020	RT	RT	···	0.98 ± 0.33	···
^{197}Au	Ag	0.55	0.68 ± 0.05	4	RT	(0.71 ± 0.05)	···	0.74 ± 0.05
	Cu	0.32	0.69 ± 0.05	80	80	0.69 ± 0.02	···	0.67 ± 0.04

[a] Extrapolated zero values (see Secs. II D1 and V C).

[b] These values were derived directly from the published impurity moments $\mu'(-1)$ and $\mu'(-2)$ (see Sec. V B 4).

[c] From a Mannheim analysis of relative f data (see Table VII).

eratures can be used best to evaluate force constant ratios at these temperatures from Mannheim's integral,[6] followed by an extrapolation to a *zero-degree* effective host-impurity force constant[12] ratio. However, due to a scarcity of host data, this method is limited to a handful of impurity systems. It was carried out[8] for Fe in Cu and Pd (see Table II).

2. Low-temperature effective host-impurity force-constant ratios

In those cases in which the phonon density of states function is not known at all or is known only at room temperature, reliable *low-temperature* effective host-impurity force-constant ratios can alternatively be obtained from a moment analysis. Impurity moments can be determined from experimentally measured f values at temperatures near that of liquid He, as well as near room temperature and above, by means of the moment expansions, Eqs. (1a) and (1c). In this way a low-temperature value for $\mu'(-1)$ and several values for $\mu'(-2)_T$, at and above room temperature, can be obtained. For many of the studied dilute alloy systems of Fe we have found $\mu'(-2)$ to be temperature dependent, varying as much as 4% per 100 K near 296 K.

As will be discussed in Sec. IV B, host moments such as $\mu(-1)$ and $\mu(-2)$ can be obtained quite accurately from a moment analysis of heat capacity data.[13] Such an analysis yields *low-temperature* moments, characteristic of about 100–150 K. In order to obtain consistent effective host-impurity force-constant ratios with the help of the impurity-to-host moment ratios derived in this work from Mannheim theory [Eqs. (12) and (15), Sec. III], it is necessary for most materials to extrapolate the experimentally obtained impurity moments $\mu'(-2)_T$ down from temperatures at and above room temperature to about 100 K. [Direct calculations of $\mu'(-2)_T$ from f data in that temperature range is restricted by the convergence criterion for the expansion, Eq. (1a).] From $\mu'(-1)$ and $\mu'(-2)$ two independent values for the low-temperature effective host-impurity force-constant ratio can be obtained, representative of about 100 K. For most metals included in this study, anharmonic effects are probably rather small at these temperatures.

If for a material (e.g., Cu) $G(\omega)_{T_0}$ is known from neutron studies at low temperatures (~100 K), the same information can, of course, be obtained independently from a fit of low-temperature to room-temperature f values to the Mannheim integral,[6] similar to the method described in Sec. II D 3.

We have calculated a set of low-temperature effective host-impurity force-constant ratios from suitable Mössbauer f values and a moment analysis of heat-capacity data for the relevant host metals (see Table II and Sec. V).

3. Pseudoharmonic effective host-impurity force-constant ratios

Most neutron-dispersion data for pure materials are available only at one temperature T_0 (usually room temperature). From these a density-of-states function $G(\omega)_{T_0}$ for that temperature can be derived, using a Born–von Kármán analysis. A precision measurement of the Mössbauer $f(T_0)$ value at the same temperature T_0, analyzed with the help of the Mannheim integral,[6] yields a pseudoharmonic effective nearest-neighbor host-impurity force-constant ratio[12] $(A/A')_{T_0}$. $f(T)$ values for temperatures in a small range above and below T_0 should be included in the fit to the Mannheim integral only if a correction for anharmonicity of the form $\langle x^2\rangle_T = \langle x^2\rangle_{T_0}[1+\epsilon(T-T_0)]$ is applied.[8,10] The traditional analysis of f values measured over a large temperature range and using a correction term $(1+\epsilon T)$ does not properly account for the temperature dependence of $G(\omega)$ for the host,[8] and the interpretation of the resulting values of $\langle x^2\rangle_T$ is more ambiguous than those obtained by the above procedure. We have, therefore, reanalyzed previously published impurity data in order to obtain a more reliable set of force constant ratios (see Table II).

III. IMPURITY-HOST MOMENT RELATIONS FROM THE MANNHEIM MODEL

A. Even moments

The Mannheim model[6] for an isolated impurity is based on a cubic lattice with central forces only, where the changes in the impurity-lattice interactions are limited to nearest neighbors. The relationship between the pure-lattice phonon density-of-states function and the impurity dynamic-response function is given by[4,6,8]

$$G'(\omega) = G(\omega)(M/M')\{[1+\rho(\omega)S(\omega)]^2 + [\tfrac{1}{2}\pi\omega G(\omega)\rho(\omega)]^2\}^{-1} + \delta(\omega-\omega_L)(M/M') \times \{\rho^2(\omega)T(\omega) + (M/M') - [1+\rho(\omega)]^2\}^{-1}, \tag{10a}$$

where

$$\rho(\omega) = (M/M') - 1 + \omega^2[1-(A/A')]/\mu(+2), \tag{10b}$$

$$S(\omega) = \mathcal{P}\int_0^\infty \omega'^2(\omega'^2-\omega^2)^{-1}G(\omega')\,d\omega', \tag{10c}$$

$$T(\omega) = \omega^4 \int_0^\infty (\omega'^2 - \omega^2)^{-2} G(\omega')\, d\omega', \qquad (10d)$$

and $\delta(\omega - \omega_L)$ is the Dirac δ function at the localized mode frequency ω_L, provided a localized mode $\omega_L > \omega_{\max}$ exists [for which $1 + \rho(\omega_L)S(\omega_L) = 0$].

It should be noted that our equation (10b) differs from the definition of $\rho(\omega)$ as given by Mannheim,[6] where the approximation (valid only in the strict nearest-neighbor model) $\mu(+2) = \lambda_{xx}(0, 0)/M \equiv \frac{1}{2}\omega_{\max}^2$ was used to define λ. When, for a real material, $\mu(+2)$ is determined from a complete Born–von Kármán analysis of neutron-dispersion measurements, $M\mu(+2)$ contains contributions from nearest up to sixth or seventh neighbors. We have therefore defined $A = A_{xx}(0, 0) = M\mu(+2)$, [Eqs. (3a) and (3b), Sec. II B], as the *effective host-host force constant*. From columns 3 and 4 of Table I it can be seen that $\frac{1}{2}\omega_{\max}^2$ may be as much as 25% larger than A/M in fcc metals or 13% smaller than A/M in bcc metals. When comparing our values of A/A', as summarized in Table II with force-constant ratios λ/λ' obtained in other studies from Mannheim's original expression[6] for $\rho(\omega)$, the following conversion relation should be applied:

$$A/A' = 1 - [2\mu(+2)/\omega_{\max}^2][1 - (\lambda/\lambda')]. \qquad (10e)$$

From Eq. (10a) impurity-site moments $\mu'(n)$ can be calculated [for a given impurity mass and any given host-phonon distribution function $G(\omega)$] as a function of the force-constant ratio A/A' which appears in $\rho(\omega)$. Such numerical calculations were performed for a number of host-distribution functions and a limited range of values of M/M' and A/A' (see Figs. 1 and 2 and Sec. III B).

In the Appendix we derive exact functional relationships for the ratios of nth impurity site moments to host moments, for even n, using the approximations of the Mannheim impurity model.[6] We find [Eq. (A17)],

$$\frac{\mu'(+2)}{\mu(+2)} = \left(\frac{M}{M'}\right)\left(\frac{A'}{A}\right). \qquad (11)$$

Note that this relation is consistent with our definitions of $\mu(+2)$ and $\mu'(+2)$, Eqs. (3a) and (3d). We also derive an analytical expression for $\mu'(+4)/\mu(+4)$ in the Appendix [Eq. (A19)]. Of greater usefulness is the ratio [Eq. (A20)]

$$\frac{\mu'(-2)}{\mu(-2)} = \left(\frac{M'}{M}\right)\left[1 - \beta_{-2}\left(1 - \frac{A}{A'}\right)\right]. \qquad (12)$$

It should be noted that Eqs. (11) and (12) include contributions from localized modes, if present, and that they are *valid at all temperatures*.

We see that Eq. (11) agrees with Eq. (6) for the *Einstein model*,[14] but that Eq. (12) would agree only if $\beta_{-2} \equiv 1$. In Table I, we have calculated the values of β_{-2} for a number of models of ideal lattices and for real-host materials (see Sec. IV A). Clearly, the experimental values of β_{-2} are far from unity, being instead much more nearly the $\beta_{-2} = 0.596$ value obtained for the *Leighton model*.

There is, however, a striking similarity between our relation Eq. (12) and that given by Maradudin and Flinn,[10] Eq. (8). Rewriting our expres-

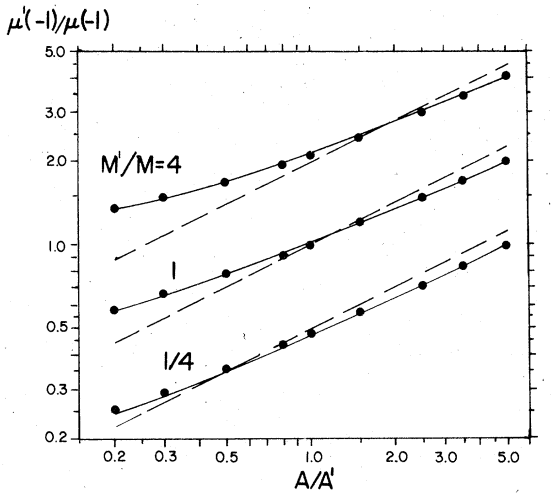

FIG. 1. ● Mannheim-model predictions of $\mu'(-1)/\mu(-1)$ (see Sec. III B) for $0.2 < A/A' < 5$ and $M'/M = 4$, 1 and $\frac{1}{4}$, using the density of states function $G(\omega)_{296}$ of Cu, representative of fcc metals. The *dashed lines* represent the Einstein model [Eq. (6)], while the *solid lines* represent the proposed functional relationship Eq. (15).

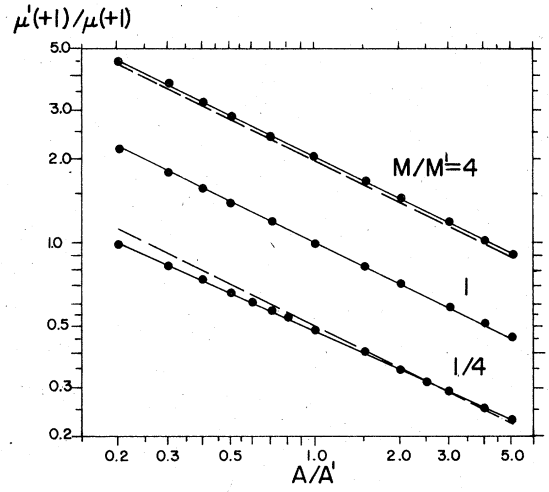

FIG. 2. ● Mannheim-model predictions of $\mu'(+1)/\mu(+1)$ (see Sec. III B) for $0.2 < A/A' < 5$ and $M/M' = 4$, 1, and $\frac{1}{4}$, using the density of states function $G(\omega)_{296}$ of Cu, representative of fcc metals. The *dashed lines* represent the Einstein model [Eq. (6)], while the *solid lines* represent the proposed functional relationship Eq. (16).

sion Eq. (12) in terms of the inverse ratio A'/A and expanding for *small* values of the quantity $[1-(A'/A)]$, we obtain

$$\frac{\mu'(-2)}{\mu(-2)}=\left(\frac{M'}{M}\right)\left[1+\beta_{-2}\left(1-\frac{A'}{A}\right)+\beta_{-2}\left(1-\frac{A'}{A}\right)^2+\cdots\right]. \quad (13)$$

The main difference between Eqs. (13) and (8) is the absence of the factor $\frac{5}{4}$ in the third term of the expansion. The discrepancy may have been introduced by the use of "Ludwig's approximation" in Maradudin and Flinn's derivation.[10]

Equation (9), which Ohashi and Kobayashi[11] have derived for Visscher's simple cubic model[9] in the high-temperature limit, functionally agrees with our Eq. (12). From direct calculation (Table I) we find, however, for the coefficient $\beta_{-2}^{sc}=0.660$ instead of the value 0.675 given in Ref. 11.

Many of the values of host-impurity force-constant ratios for dilute alloys which have appeared in the literature have been obtained[15,16] by applying the Einstein-Debye relation [Eq. (7d)] to impurity mean-squared displacement measurements at or above room temperature (see Sec. II A). By comparing the Einstein-Debye force-constant ratio at high temperatures $(\gamma'/\gamma)_{HT}$ from Eq. (7d) with the earlier defined and more meaningful effective impurity-host force-constant ratio A'/A from Eq. (12), the magnitude of possible errors due to the use of this crude model becomes apparent. Assuming that the appropriate Debye temperature $\Theta_D(-2)$ for the host has been used (this is the exception rather than the rule), we have

$$A'/A=(\gamma'/\gamma)_{HT}\{(1/\beta_{-2})-[(1/\beta_{-2})-1]\times(\gamma'/\gamma)_{HT}\}^{-1}, \quad (14)$$

where we have used $\mu(-2)/\mu'(-2)=[\Theta_D'(-2)/\Theta_D(-2)]^2$ [see Eq. (7b)].

In Columns 1 and 2 of Table III we give the values of A'/A from Eq. (14) for several values of $(\gamma'/\gamma)_{HT}$, using an average value for β_{-2} for cubic metals of 0.57. It is obvious that the use of Eq. (7d) instead of Eq. (12) can lead to substantial errors when applied to high-temperature impurity measurements, quite apart from the complications of anharmonicity.

TABLE III. Relation between Einstein-Debye force-constant ratios [Eq. (7d)] and effective impurity-host force-constant ratios as obtained from Mössbauer f measurements (Secs. III A and III B).

High temperature		Low temperature	
γ'/γ_{HT} [a]	A'/A [b]	γ'/γ_{LT} [c]	A'/A [d]
2.0	8.2	2.0	1.9–3.5
1.5	2.4	1.5	1.4–2.2
1.3	1.7	1.3	1.2–1.7
1.0	1.0	1.0	1.06–0.92
0.70	0.57	0.70	0.59–0.71
0.50	0.36	0.50	0.41–0.46
0.30	0.20	0.30	0.24–0.25

[a] From application of Eq. (7d) to high-temperature Mössbauer fraction measurements.

[b] From Eq. (14), using $(\beta_{-2})_{av}=0.57$.

[c] From application of Eq. (7d) to low-temperature Mössbauer fraction measurements.

[d] From Eq. (17), using $(\beta_{-1})_{av}=0.85$ and $(\beta_{+4})_{av}=0.8$. The two limits are for $M'/M=\frac{1}{4}$ and $M'/M=4$, respectively.

B. Odd moments

Attempts to derive from the Mannheim model[6] functional relationships in a closed form, similar to Eqs. (11) and (12) for the experimentally and theoretically important impurity-site moments $\mu'(-1)$ and $\mu'(+1)$, were not successful. Rather than describing the impurity motion near the classical limits, as do the even moments [see Eqs. (1a) and (1b)], these odd moments characterize the zero-point motions of the impurity [see Eqs. (1c) and (1d)]. As an alternative we have computed $\mu'(-1)/\mu(-1)$ and $\mu'(+1)/\mu(+1)$ *numerically* from the Mannheim dynamic response function $G'(\omega)$ [using Eqs. (2a), (2b), and (10a)] for a range of values $0.25\leq M'/M\leq 4$ and $0.2\leq A/A'\leq 5$, and using the density of states functions for various host materials listed in Table I. The latter were derived from neutron-dispersion measurements (see references to Table I). In Figs. 1 and 2 the circles represent these calculations using $G(\omega)_{T_0}$ for Cu at room temperature.[17] The dashed lines show the predictions of the Einstein model, Eq. (6), while the solid lines represent the following functional relations (Fig. 1):

$$\frac{\mu'(-1)}{\mu(-1)}\simeq\left(\frac{M'}{M}\right)^{(1/2)+a}\left\{1-\left(\frac{M'}{M}\right)^{-2a}\beta_4\left[1-\left(\frac{A}{A'}\right)^{1/2}\right]\right\}, \quad (15)$$

with $a=\frac{1}{2}(1/\sqrt{\beta_{-1}}-1)=0.043$. The values of β_{-1} and $\beta_4=0.779$ are those for Cu from Table I. Also (Fig. 2)

$$\frac{\mu'(+1)}{\mu(+1)}\simeq\left(\frac{M}{M'}\right)^{(1/2)+b}\left(\frac{A'}{A}\right)^{1/2[1-b(M'/M)]}, \quad (16)$$

with $b=\frac{1}{2}(\beta_1-1)=0.021$ from Table I.

The following observations can be made regarding Eqs. (15) and (16) and Figs. 1 and 2.

(i) For the chosen range of mass and force-constant changes the functions Eqs. (15) and (16) represent the direct calculations from integration of the Mannheim dynamic response function [Eqs. (2) and (10)] very well indeed. The deviations reach at

most 5% near the extremes of the ranges calculated. {Improved fits could be obtained by including higher-order terms in $[1-(A/A')^{1/2}]$ and $[1-(M'/M)^{1/2}]$.}

(ii) The functional forms of Eqs. (15) and (16) were in part guessed at by comparing them with the exact functions for $\mu'(2)/\mu(2)$ [Eq. (11)] and $\mu'(-2)/\mu(-2)$ [Eq. (12)]. Approximate functional dependencies of the (−1) and (+1) moments on mass and force-constant changes have previously been discussed by Housley and Hess,[7] whose results are consistent with Eqs. (11), (12), (15), and (16). The appearance of β_4 in Eq. (15) can only be justified by its *numerical* value (Table I) since no analytical expression could be derived directly from the theoretical model. However, when we use computer fitting of the functional forms Eq. (15) and (16) to determine *best values* for the parameters a, b, and β_4 for a variety of hosts, a positive correlation appears to exist between these best values and those based on the actual host parameters β_{-1}, β_1, and β_4 as listed in Table I. Additional support for our choice of relating the small corrections a and b in the exponents of the mass terms in Eqs. (15) and (16) to the host moment ratios β_{-1} and β_{+1}, respectively, comes from an early perturbation analysis by Lipkin.[18] He showed that for an *isotopic impurity* $(A/A'\equiv 1)$ at $T=0$, the slope of $\ln[\mu'(-1)/\mu(-1)]$ vs $\ln(M'/M)$ for small mass changes deviates a few percent from the value $\frac{1}{2}$ which would be expected from the *Einstein model*, Eq. (6). He also showed that this deviation is related to a weighted average frequency of the host. Alternatively, our results for the (−1) moment ratio may also be compared to the low-temperature results of a calculation by Dawber and Elliott[19] for an *isotopic impurity* $(A/A'\equiv 1)$. We find from Mannheim's theory[6] and the density-of-states function for Cu, using Eq. (15), $\log_{10}[\mu'(-1)/\mu(-1)]/\log_{10}(M'/M)=\frac{1}{2}(\beta_{-1})^{-1/2}=0.543$. Dawber and Elliott,[19] using a *Debye distribution*, found for the same coefficient the value 0.478, which differs from our value $\frac{1}{2}(\beta^D_{-1})^{-1/2}=0.539$ from Table I.

(iii) As does the relation for the Einstein model [Eq. (6)], our Eq. (16) based on Mannheim's model, shows a linear relation between $\log_{10}[\mu'(+1)/\mu(+1)]$ and $\log_{10}(A/A')$ [and with $\log_{10}(M'/M)$ as well] except for a small change in slope (see Fig. 2). This shows that the Einstein-Debye relation Eq. (7d) adequately describes the (+1) moment ratio. Unfortunately, these moments are more difficult to obtain experimentally with sufficient reliability to determine accurate force constant ratios (see Sec. VI).

(iv) The ratio $\mu'(-1)/\mu(-1)$ deviates considerably from that predicted by the Einstein model [see Eq. (15) and Fig. 1]. Consequently, if Eq. (7d) is used to obtain an Einstein-Debye force-constant ratio $(\gamma'/\gamma)_{LT}$ from low-temperature Mössbauer fraction measurements (see Sec. II C 2), it can differ appreciably from the more meaningful effective impurity-host force-constant ratio A'/A defined above (Sec. II B). From Eqs. (7d) and (15), using $\mu(-1)/\mu'(-1)=\Theta'_D(-1)/\Theta_D(-1)$ [see Eq. (7b)], we have

$$A'/A=(\gamma'/\gamma)\{(1/\beta_4)(M'/M)^a+(\gamma'/\gamma)^{1/2}\times[1-(1/\beta_4)(M'/M)^{2a}]\}^{-2}. \quad (17)$$

In columns 3 and 4 of Table III we illustrate the systematic errors which can be introduced by an inappropriate use of the Einstein-Debye relation Eq. (7d) to interpret low-temperature f measurements. In particular, Table III shows that for both low- and high-temperature impurity f data, the simplified model erroneously *compresses* the apparent range of effective force-constant ratios (see Sec. I A and Sec. VI B). This effect is probably partly responsible for the earlier conclusions about the approximate validity of the isotopic impurity theory.[1-3] In Sec. V, Table II, we have re-evaluated earlier precision f data[16] which had been analyzed using Eq. (7d).

C. Summary

In Table IV we summarize the most useful moment relationships from the Mannheim model,[6] expressing effective host-impurity force-constant ratios as functions of impurity-site moment to host moment and mass ratios by solving Eqs. (11), (12), (15), and (16) for A/A'. In particular, since $\mu'(-1)$ and $\mu'(-2)$ are easily obtainable from precision Mössbauer fraction measurements (see Secs. II A and II D 2), the first two relations, in combination with values of $\mu(-1)$ and $\mu(-2)$ for the host material, determine two independent values for the effective host-impurity force-constant ratio A/A' (see Sec. V).

IV. MOMENTS AND MOMENT RATIOS IN MODEL LATTICES AND IN CUBIC METALS AND RARE-GAS SOLIDS

A. Moments from neutron-dispersion data

As we have seen in Sec. III, the moment ratios β_n appear in the expressions for determining force-constant changes due to impurities. In an effort to investigate the characteristics of these β_n, we have determined the moments for a number of lattice models and cubic-host materials. Several of these β_n are listed in Table I. The moments were numerically calculated from weighted sums over phonon distributions obtained from Born-von Kármán model fits to dispersion relations. We have

TABLE IV. Effective host-impurity force constant ratios A/A' from impurity site to host moment ratios (Mannheim theory) (Sec. III).

Moment ratio n	Force-constant ratio A/A'	Use	Remarks [a]
-2	$\left[1+(\beta_{-2})^{-1}\left(\frac{\mu'(-2)}{\mu(-2)}\frac{M}{M'}-1\right)\right]$	High-temperature f measurements	Exact [b]
-1	$\left\{1+(\beta_4)^{-1}\left(\frac{M'}{M}\right)^{2a}\left[\frac{\mu'(-1)}{\mu(-1)}\left(\frac{M}{M'}\right)^{(1/2)+a}-1\right]\right\}^2$	Low temperature f measurements	$a\simeq\frac{1}{2}[(\beta_{-1})^{-1/2}-1]$ Approximate [c]
$+1$	$\left[\frac{\mu(+1)}{\mu'(+1)}\left(\frac{M}{M'}\right)^{(1/2)+b}\right]^{2/[1-b(M'/M)]}$	Low temperature thermal shift	$b\simeq\frac{1}{2}[\beta_1-1]$ Approximate [c]
$+2$	$\frac{\mu(+2)}{\mu'(+2)}\frac{M}{M'}$	Correction to high temperature shift	Exact [b]

[a] The host parameters β_n are defined in Eq. (4).
[b] See Appendix.
[c] See Sec. III B.

used the inelastic neutron scattering data published by the authors referenced in Table I. In order to obtain compatible moment ratios, all materials were analyzed uniformly with Born–von Kármán models employing general forces and including sixth nearest neighbors for fcc and seventh nearest neighbors for bcc lattices. The elastic constants, preferably for the same temperature as that of the neutron measurements, were included as parameters to the fit to obtain a more reliable representation of the low frequencies, to which the β_n for negative n are rather sensitive. The criterion of best fit to the dispersion data was identical in all cases. The phonon density-of-states function $G(\omega)$ was calculated by direct summation over a fine grid in $\vec{k}$ space.

B. Moments from heat-capacity analysis

In order to compare the consistency of our moment calculations from neutron-dispersion data with those obtainable from an analysis of heat-capacity data, we have analyzed such data for all nonferromagnetic metal hosts listed in our summary Table II. The methods of heat-capacity analysis have been treated extensively in the literature.[13,20] The overall accuracy of the moment analysis has been estimated to be that of the heat-capacity data (2%–3%).[13] The corrections for electronic contributions to the heat capacity and the conversion from the measured C_P to C_V have been made with appropriate care, and uniform convergence criteria were applied to the numerical integrations of the series expansions.[13] Since the principal contributions to the heat-capacity integral for most metals investigated here comes from the data between 50 and 150 K, the negative as well as the positive moments calculated in this analysis can be considered to be representative of a low-temperature phonon-distribution function $G(\omega)$ with T about 100–150 K.

C. Comparison between neutron and heat-capacity data

In Table V we compare moments which were obtained by us from neutron as well as from heat-capacity data for Cu, Al, and Pt for which comparable data are available in the literature. For the neutron data the excellent agreement illustrates the fact that the frequency moments are not sensitive to the particular Born–von Kármán force model used in our calculations. The variation in the listed values of a few tenth of a percent for most moments [except $\omega_D(-3)$ which is determined by the *initial* curvature of $G(\omega)$] is an indication of the accuracy of these data. The somewhat larger deviations in the values of $\omega_D(-3)$ probably represent the relatively greater weight we accorded to the elastic constants in our neutron-data fitting procedure.

For the evaluation of moments from heat-capacity analysis we made use of some recent critical compilations of such data.[21–23] The stated errors are those derived from the fitting routine. They do not include systematic uncertainties. If the latter are estimated to be a few percent,[13] then all values listed are consistent with each other. In particular, the use of recent smoothed average heat-capacity data[23] for platinum leads to a reduction of the earlier noted discrepancy between the heat-capacity data on the one hand, and neutron dispersion, elastic constant, and Mössbauer measurements on Pt on the other hand,[24]

TABLE V. Comparison between frequency moments from dispersion relations and heat-capacity data (Sec. IV C).

Metal (temp.)	n	$\omega(n)=\mu(n)^{1/n}$ ($\times 10^{13}$ rad/sec) From neutron-scattering data			From heat-capacity data		
		This work and Ref. a	Ref. b	Ref. c			
	+4	3.38	3.37	3.39			
Cu	+2	3.18	3.18	3.20			
(296 K)	+1	3.05	3.04	3.07			
	−1	2.69	2.69	2.72			
	−2	2.37	2.37	2.39			
	$\omega_D(-3)$	4.30	4.36	4.34			
		This work and Ref. e		Ref. c	This work and Ref. f	Ref. d	Ref. g
	+4	3.45		3.41	3.38 ± 0.04		3.41 ± 0.02
Cu	+2	3.29		3.21	3.21 ± 0.03		3.24 ± 0.01
(80 K)	+1	3.11		3.10	...		...
	−1	2.75		2.76	2.72 ± 0.02		2.76 ± 0.01
	−2	2.42		2.43	2.43 ± 0.02		2.43 ± 0.01
	$\omega_D(-3)$	4.47		4.52	...	4.49	4.52 ± 0.01
		This work and Ref. h	(80 K)	Ref. h (300 K)	Ref. f	Ref. d	Ref. h
	+4	4.41	4.43	4.34	4.27 ± 0.04		4.36 ± 0.13
Al	+2	4.11	4.13	4.03	4.06 ± 0.02		4.08 ± 0.01
(80 K)	+1	3.93	...	...	...		...
	−1	3.47	3.47	3.35	3.39 ± 0.03		3.45 ± 0.01
	−2	3.07	3.06	2.94	3.09 ± 0.03		3.05 ± 0.01
	$\omega_D(-3)$	5.77	5.66	5.37	...	5.61	5.63 ± 0.01
		This work and Ref. i			Ref. j	Ref. d	Ref. k
	+4	2.60			2.80 ± 0.02		2.93 ± 0.11
Pt	+2	2.42			2.52 ± 0.01		2.60 ± 0.05
(90 K)	+1	2.30					2.41 ± 0.04
	−1	1.99			1.99 ± 0.02		2.01 ± 0.03
	−2	1.72			1.72 ± 0.02		1.73 ± 0.02
	$\omega_D(-3)$	3.05			...	3.07	3.12 ± 0.03
		From x-ray diffuse scattering					
		This work and Ref. l			Ref. g		
	+4	3.68			4.35 ± 0.03		
V	+2	3.54			4.13 ± 0.03		
(296 K)	+1	3.44			3.98 ± 0.03		
	−1	3.15			3.49 ± 0.03		
	−2	2.81			2.98 ± 0.02		
	$\omega_D(-3)$	5.13			5.22 ± 0.04		

[a] Reference 17.
[b] E. C. Svensson, B. N. Brockhouse, and J. M. Rowe, Phys. Rev. 155, 619 (1967).
[c] R. M. Nicklow, G. Gilat, H. G. Smith, L. J. Raubenheimer, and M. K. Wilkinson, Phys. Rev. 164, 922 (1967).
[d] Reference 22.
[e] G. Nilsson and S. Rolandson, Phys. Rev. B 7, 2393 (1973).
[f] From the heat capacity measurements of W. F. Giaugue, and P. F. Meads, J. Am. Chem. Soc. 63, 1897 (1941).
[g] Reference 25.
[h] G. Gilat and R. M. Nicklow, Phys. Rev. 143, 487 (1966).
[i] D. H. Dutton, B. N. Brockhouse, and A. P. Miiller, Can. J. Phys. 50, 2915 (1972).
[j] Reference 23.
[k] Reference 20.
[l] Reference 26.

TABLE VI. Summary of selected Mössbauer f values for ^{57}Fe impurities in cubic metals (Secs. V B 1–V B 3).

Host	T	Γ/Γ_0 [a]	$f(T)$ [b]	Ref.	Best value [c] $f(T)$
Ag	RT	?	(0.64 ± 0.04) [d]	e	
		?	(0.52 ± 0.03) [d]	f	
		?	(0.58 ± 0.03) [d]	g	...
Al	RT	?	(0.54 ± 0.02) [d]	e	
		>2	(0.52 ± 0.05) [d]	h	
		1.3	0.50 ± 0.05	i	0.50 ± 0.05
Au	RT	1.9	(0.598 ± 0.014)	j [d]	
		?	(0.62 ± 0.05)	g [d]	
		1.4	0.583 ± 0.010	k [d]	0.583 ± 0.010
Cr	RT	?	0.76 ± 0.02	g	
		1.3	0.792 ± 0.009	l	0.790 ± 0.009
Cu	RT	1.0	0.710 ± 0.014	m	
		1.5	0.727 ± 0.016	j	
		?	0.725 ± 0.034	e	
		?	0.710 ± 0.010	n	
		1.0	0.709 ± 0.006	o	
		1.0	0.703 ± 0.007	p	
		1.0	0.710 ± 0.006	q, r	0.709 ± 0.005
	4 K	1.5	0.917 ± 0.019	j	
		(1.0)	0.910 ± 0.007	g	
		(1.0)	0.911 ± 0.006	q	0.911 ± 0.005
Ir	RT	3.8	(0.807 ± 0.025)	j [d]	
		?	0.79 ± 0.03	g [d]	
		1.3	0.812 ± 0.005	r	0.812 ± 0.005
	4 K	(1.3)	0.914 ± 0.005	r	0.914 ± 0.005
Mo	RT	?	0.78 ± 0.05	e	
		?	0.76 ± 0.03	g	
		?	0.77 ± 0.01	s	
		?	0.753 ± 0.008	t	
		?	0.773 ± 0.011	u [d]	0.763 ± 0.011
	4 K	?	0.907 ± 0.010	t	
		?	(0.885 ± 0.011)	u [d]	0.907 ± 0.010
Nb	RT	?	0.63 ± 0.03	g	
		1.6	0.659 ± 0.008	w	
		?	0.660 ± 0.010	u [d]	
		1.4	0.644 ± 0.004	r	0.648 ± 0.014
	4 K	(1.4)	(0.881 ± 0.006)	r	
		?	(0.846 ± 0.010)	u [d]	0.881 ± 0.010
Ni	RT	1.1	0.80 ± 0.01	n	
		?	0.81 ± 0.05	g	0.80 ± 0.01
Pd	RT	?	0.652 ± 0.036	e	
		1.7	0.652 ± 0.015	j	
		1.1	0.661 ± 0.006	q	
		?	0.657 ± 0.024	g	0.659 ± 0.004
	4 K	?	(0.813 ± 0.013)	j [Δ]	
	13 K	?	(0.875 ± 0.015)	q [Δ]	
	20 K	(1.1)	0.891 ± 0.006	q	0.891 ± 0.010
Pt	RT	?	0.729 ± 0.025	e	
		?	0.723 ± 0.036	v	
		1.7	0.729 ± 0.016	j	
		1.1	0.723 ± 0.008	q	0.725 ± 0.007
	4 K	?	(0.85 ± 0.05)	j [Δ]	
	12 K	?	(0.897 ± 0.010)	q [Δ]	
	20 K	(1.1)	0.905 ± 0.008	q	0.905 ± 0.008

TABLE VI. (*Continued*)

Host	T	Γ/Γ_0 [a]	$f(T)$ [b]	Ref.	Best value [c] $f(T)$
Rh	RT	>2.1	0.785 ± 0.017	j	
		?	0.783 ± 0.025	g	
		?	0.78 ± 0.01	s	
		1.2	0.781 ± 0.005	r	0.718 ± 0.005
	4 K	1.9	0.875 ± 0.018	j	
		(1.2)	0.910 ± 0.006	r	0.906 ± 0.006
Ta	RT	?	(0.77 ± 0.04)	e	
		?	(0.76 ± 0.03)	g	
		?	0.704 ± 0.008	u	0.704 ± 0.008
	4 K	?	0.887 ± 0.012	u	0.887 ± 0.012
V	RT	?	(0.55 ± 0.03)	e	
		?	(0.76 ± 0.03)	g	
		?	(0.547 ± 0.024)	x	
		?	(0.76 ± 0.01)	y	
		?	(0.70 ± 0.01)	s	...
	4 K	?	(0.913 ± 0.010)	u	...
W	RT	?	(0.86 ± 0.03)	e	
		?	(0.86 ± 0.05)	g	
		?	0.797 ± 0.009	u	0.797 ± 0.009
	4 K	?	0.916 ± 0.013	u	0.916 ± 0.013

[a] Experimental linewidth at half maximum (see Sec. V B 2).

[b] Errors include statistical plus estimated systematic errors (e.g., "black absorber" corrections) where known (see Sec. V B 2).

[c] See Secs. V B 2 and V B 3 for criteria used.

[d] May not represent substitutional sites only or other uncertainties.

[e] J. Bara and A. Z. Hrynkiewicz, Phys. Status Solidi 15, 205 (1966).

[f] J. W. Burton and R. P. Goodwin, Phys. Rev. 158, 218 (1967).

[g] Reference 2. ([d] May not represent substitutional sites only.)

[h] C. Janot and H. Gibert, Philos. Mag. 27, 545 (1973). ([d] may not represent substitutional sites only.)

[i] References 4 and 31.

[j] Reference 15. ([d] Γ/Γ_0 suggests admixture of nonsubstitional sites; Δ values uncertain due to magnetic splitting.)

[k] Reference 30. ([d] may have small admixture of nonsubstitutional sites.)

[l] B. F. Brace, D. G. Howard, and R. H. Nussbaum, Phys. Lett. 43A, 336 (1973).

[m] R. M. Housley, J. G. Dash, and R. H. Nussbaum, Phys. Rev. 136, A464 (1964).

[n] D. G. Howard and J. G. Dash, J. Appl. Phys. 38, 991 (1967).

[o] D. L. Sprague, see Ref. 16.

[p] D. P. Johnson and J. G. Dash, Phys. Rev. 172, 983 (1968).

[q] Reference 16. (Δ values uncertain due to magnetic splitting.)

[r] This work.

[s] D. A. O'Connor, M. W. Reeks, and G. Skyrme, J. Phys. F 2, 1179 (1972). (These are absorber f values.)

[t] Reference 37.

[u] Reference 27 and private communication with authors. ([d] values uncertain due to x-ray background.)

[v] R. M. Housely, N. E. Erickson, and J. G. Dash, Nucl. Instrum. Methods 27, 29 (1964).

[w] Reference 4.

[x] J. A. Moyzis, Jr., G. de Pasquali, and H. G. Drickamer, Phys. Rev. 172, 665 (1968).

[y] A. Simopoulos and I. Pelah, J. Chem. Phys. 51, 5691 (1969).

suggesting possible systematic errors in the C_P data. The case of Pt represents the worst discrepancy between moments derived from heat capacities and those from neutron-dispersion data for all host metals listed in Table II. For comparison we have also included in Table V the "best" values chosen by Phillips[22] for $\omega_D(-3)$ from a critical review of C_P data.

Since the neutron cross section of vanadium is nearly totally incoherent, conventional neutron diffraction cannot be applied to study the dispersion relations of V. Moments for V as listed in Table V are those obtained from heat capacities[25] and those derived from x-ray dispersion curves[26] using a Born–von Kármán model fit described in Sec. IV A. As can be seen, the two negative moments are within 10% of each other. However, the positive moments are in substantial disagreement. The reason for this discrepancy remains unresolved at this time. It is therefore not possible to confidently use an effective host-host force constant for the interpretation of Mössbauer impurity studies in V.[1,2,27]

D. Moment ratios and characteristic trends in face-centered-cubic metals and rare-gas solids

In Table I we have listed moment ratios β_n [Eq. (4)] resulting from our analysis of coherent inelastic neutron scattering measurements (see Sec. IV A). We also include the values of $A/M = \mu(+2)$ and $\frac{1}{2}\omega_{\max}^2$ for comparison (see Sec. III A), as well as the elastic constants which were used in the fitting of the dispersion data. Some interesting regularities can be observed.

Under the assumption of pure nearest-neighbor central forces, the only stable lattice is face-centered cubic; this is the so-called *Leighton* model. Qualitatively, it predicts the general features of the dispersion relations and the phonon density of states quite well. The model constraints on the elastic constants are such that $C_{44} = C_{12} = \frac{1}{2}C_{11}$. For a metal lattice to display such a relationship between elastic constants does not, however, guarantee that the interaction need be purely central or nearest neighbor, though a departure from this relationship clearly indicates departure from the nearest-neighbor central interaction. This is because the elastic constants are sensitive only to the low-frequency phonons.

The parameter β_{-2} is a combination of $\mu(-2)$, which is sensitive to low frequencies, and $\mu(+2)$, which is sensitive to high frequencies, and therefore gives additional information about the interaction. In general, β_{-2} is smaller than that predicted by the Leighton model, indicating that for most metals the higher-frequency modes tend to be shifted upward with relation to the lower-frequency modes over what the Leighton model would predict. This tendency generally increases with increasing atomic mass.

By both criteria, nickel appears to be the material closest to the ideal nearest-neighbor central interaction. The noble gases have elastic constants near the ideal ratio, but have considerably smaller β_{-2}. On the other hand, the values of β_{-2} and β_{-1} derived for Rh and Ir from heat-capacity data (no neutron studies available) are virtually the same and both are anomalously high relative to other fcc metals and the Leighton model. Yet, the elastic constants for Ir are close to the "ideal" relationship. Neutron-dispersion measurements would be very helpful for an analysis of this anomaly.

With the exception of Rh and Ir, as discussed above, the fcc lattices, as listed in Table I, show a surprisingly small spread of values for each β_n in spite of changes in the characteristic frequency $(A/M)^{1/2}$ by almost an order of magnitude.

E. Moment ratios and characteristic trends in body-centered-cubic metals

For a body-centered-cubic lattice, assuming nearest-neighbor central forces only, the prediction for the elastic constants is $C_{44} = C_{12} = C_{11}$. As a consequence, one of the transverse branches along [110] should have a predicted zero frequency for all wave vectors, the resulting phonon distribution should have a peak at zero frequency, and the negative-frequency moments should become infinite, causing $\beta_n \to 0$ for $n < 0$. This unphysical behavior of the nearest-neighbor model can be removed by including *either* a small amount of noncentral component to the nearest-neighbor force (in which case $C_{44} = C_{11} \neq C_{12}$) *or* a small contribution from second nearest neighbors (in which case $C_{44} = C_{12} \neq C_{11}$). In either case, the transverse phonon branch along [110], though no longer at zero frequency, remains at very low frequencies, causing the β_n for $n < 0$ to be quite small. The alkali metals, represented in Table I by Na and Rb, appear to be examples of such a slight departure from the nearest-neighbor central-force model.

For most of the bcc metals investigated, the noncentral and/or distant-neighbor contributions are not small. Fe is an example of a lattice with nearly central forces and with a large second-neighbor contribution. The elastic constants (see Table I) show $C_{11} > C_{12} \sim C_{44}$, and the resulting β_n are considerably larger (with the exception of β_{+1}) than those for Na and Rb, in fact very close to those of the Leighton model. W has proportionately a still larger contribution from the second neighbor, and the increase in the β_n is even greater. The other bcc metals investigated generally show

rather strong departure from the condition of central forces as well as contributions from more distant neighbors.

V. SUMMARY OF EFFECTIVE HOST-IMPURITY FORCE-CONSTANT RATIOS FROM MÖSSBAUER MEASUREMENTS

A. Applicability of Mannheim's impurity model to real impurity systems

Our investigation as summarized in Table I seems to indicate that the rare-gas lattices, the alkali metals, and the fcc metals of the first-transition group (Ni, Cu) are predominantly of the nearest-neighbor central-force type. Other interactions become increasingly more important in the heavier fcc metals and are clearly quite important in most bcc metals. It could therefore be concluded that Mannheim's impurity model has little value for the analysis of impurity dynamics in these latter hosts. We will present some arguments here why our method of analysis of force constant changes, though based on the Mannheim model, is nevertheless a physically meaningful approach.

(i) If Mössbauer experiments would allow an accurate determination of $\mu'(+2)$, the value of A/A' derived from Eq. (11) would be *model independent* (see Sec. II B) as shown by Housley and Hess.[7] Unfortunately, $\mu'(+2)$ appears only in the higher-order terms of Eqs. (1a) and (1b).

(ii) The accurately measurable impurity moments $\mu'(-1)$ and $\mu'(-2)$ can only be interpreted in terms of the effective restoring force ratio A/A' (see Sec. II B) through the use of Eqs. (11) and (15), both derived under the restrictions of the Mannheim model. However, we notice that for the host metals, both fcc and bcc (excluding Na and Rb), the standard deviations among the values of β_{-2} and β_{-1} are 9% and 3%, respectively, with the values for the Leighton model falling between the averages for fcc and bcc metals. Thus, we may conclude that in the pure metals the moment ratios β_{-2} and β_{-1} are only weakly model dependent. It seems therefore reasonable to assume that for the relatively small force-constant changes which we find in dilute cubic alloys, the ratios β'_{-2} and β'_{-1} for the impurity-site moments are only weakly model dependent also.

(iii) Finally, the values of A/A' obtained independently from measurements of $\mu'(-2)$ and $\mu'(-1)$ (see Table II) generally agree with each other within experimental errors. This then constitutes a test of internal consistency of the used functional relations. The deviations of the unknown "real" relations from those derived analytically from Mannheim's model must therefore be no larger than the achievable experimental accuracy.

We conclude, therefore, that within presently achievable experimental errors, Mannheim's model represents well the impurity problem in metals, in spite of its inherent drastic simplifications.

B. Summary of Mössbauer f values for ^{57}Fe, ^{119}Sn, and ^{197}Au

1. ^{57}Fe impurity systems

In Table VI we summarize a selection of reliable Mössbauer f values for ^{57}Fe from the literature. We have also included several new data from this investigation. The selection of entries was made on the basis of a combination of considerations.

(a) The data represent absolute f values with reasonable error bars.

(b) Sufficient information about methods of source or absorber preparation has been presented by the authors to support the assumption that the f values represents *substitutional* impurity sites.

(c) The experimental linewidth provides further clues in this regard. For several investigations we found a lack of information to satisfy this criterion. Data, about which we found evidence for reasonable doubt, have been entered in parentheses. They are discussed in Sec. V B 3.

(d) We have listed f values at room temperature and at low temperatures only (where available) because of their special role in this method of analysis (see Sec. II D).

For values of $f(T)$ at other temperatures we refer the reader to the listed references. For a few hosts for which data are available at other than room temperature, we used in our analysis f values at nearby temperatures. The temperatures representative for the data used in the force constant analysis are listed in Table II.

A more complete listing of all published $f(T)$ values through 1968 has been prepared by Bara.[28] More recent data can be found in the *Mössbauer-Effective Data Index*.[29]

2. Discussion of column listings of Table VI

In addition to listing the host metal and the temperature in the first two columns, we list in the third column the *line broadening* of source or absorber, whichever the f value refers to. The ratio Γ/Γ_0 was deduced, where possible, from the information given by the authors, assuming $\Gamma_0 = 0.100$ mm/sec and subtracting from the combined experimental linewidth of source and absorber the width of the absorber used in source studies or of the source in absorber studies. Thus the parameter Γ/Γ_0 contains both source (absorber) broadening and instrumental broadening effects. It should

be clear that in all cases where such information is not available (indicated by a question mark) or where Mössbauer spectra appear to be excessively broadened, the listed f values may not represent impurity atoms in uniform substitutional sites. In all those cases an evaluation in terms of effective force-constant changes must be considered as tentative. Where the values of Γ/Γ_0 appear in parentheses, the line shapes were measured only at room temperature and it was assumed that the linewidth did not change with T. Consistency between high and low temperature f values supported this assumption.

In column 4 we list the f values selected on the basis of the above considerations. The stated errors include both statistical and systematic uncertainties, where given by the authors (e.g., blackness correction for black-wide absorbers). The references in column 5 to the original papers include for source cases special footnotes related to the reliability of individual measurements.

In column 6 we list a set of "most reliable" f values which we have used to calculate effective host-impurity force-constant ratios (Table II). These values are weighted averages of the data of column 4, excluding those in parentheses for the reasons given in the footnotes to the table and in Sec. V B 3. The quoted errors are compromises between the errors of the most precise data and the standard deviations for the group. Where the discrepancies between published data could not be reconciled, we do not list a value in column 6.

3. ^{57}Fe-impurity systems with special problems

In metals for which there exists a large discrepancy between the size of the impurity atom and the atomic volume of the host lattice, substitutional sites have been found to be thermodynamically unstable. In particular, in Al and Au two types of stable sites have been identified for Co/Fe impurities.[4,30,31] Recent preliminary experiments in our laboratory on sources of Co^{57} in Ag, which has lattice spacings comparable to those in Al and Au, indicate similar problems. No linewidths have been reported for any of the f studies listed for this host.

Another group of metals which presents metallurgical problems in the preparation of single-line Mössbauer sources is the group of bcc metals Mo, Nb, Ta, V, and W. Except for Nb, authors reporting f measurements have not published their linewidths. The various room-temperature f values for V, in particular, are mutually inconsistent. The recently published low-temperature f measurements[27] would be consistent with one of the room temperature f values of 0.70; however, this f value seems to be inconsistent with the same author's thermal shift measurements.[27] In fact, V is extremely reactive with small quantities of impurity gases at elevated temperatures, including hydrogen. The latter gas, which is often used to reduce the $^{57}CoCl_2$ radioactive deposit on the sample, is known to substantially change the Mössbauer fraction.[32] In view of these unresolved problems for the ^{57}Fe-V system, as well as the problems for pure V (Sec. IV C), we do not include V in our force-constant analysis. Also, the recently published f values for W and Ta at room and at low temperatures[27] are quite different from formerly published f values at room temperature. Unfortunately, these recent and more precise data for ^{57}Fe in Ta and W are not supported by published linewidths.

4. ^{119}Sn impurity systems

Data for ^{119}Sn in various host metals are generally less accurate as a group. Also, all these stud-

TABLE VII. Summary of Mössbauer f values for ^{119}Sn and ^{197}Au impurities in cubic metal absorbers (see Secs. V B 4 and V B 5).

Impurity	at.%	Host	T	$f(T)$	Ref.
^{119}Sn	1	Ag	RT	0.27 ± 0.01	a,b
			4 K	0.80 ± 0.02	a
	<2	Au	RT	0.30 ± 0.03	b,c
			4 K	0.85 ± 0.02	c
	1	Pb	4 K	0.80 ± 0.06	d
	?	Pd	4 K–750 K	$\mu'(n)$ analysis	e
	1	Pd	4 K–RT	relative f's $f_{4K}/f_{RT} = 2.1 \pm 0.1$	f
	<3	Pt	RT	0.53 ± 0.03	b
	<3	V	RT	0.46 ± 0.03	b
^{197}Au	5	Ag	4 K	0.195 ± 0.008	g
	2	Cu	4 K	0.239 ± 0.003	g
			80 K	0.071 ± 0.003	g

[a] O. P. Balkashin and V. V. Chekin, Fiz. Tverd. Tela. 12, 3597 (1971) [Sov. Phys. Solid State 12, 2919 (1971)].

[b] V. A. Bryukhanov, N. N. Delyagin, and V. S. Shpinel', Zh. Eksp. Teor. Fiz. 47, 80 (1964) [Sov. Phys. JETP 20, 55 (1965)].

[c] V. V. Chekin, A. I. Velikodnyi, S. N. Glushko, and Ye. D. Semenova, Fiz. Met. Metalloved. 33, 781 (1972) [Phys. Met. Metallogr. 33, 102 (1972)].

[d] S. N. Glushko, V. V. Chekin, A. I. Velikodnyi, and L. F. Rybal'chenko, Zh. Eksp. Teor. Fiz. 62, 661 (1972) [Sov. Phys. JETP 35, 349 (1972)].

[e] R. K. Puri, Phys. Status Solidi B 70, 785 (1975).

[f] G. van Landuyt, C. W. Kimball, and F. Y. Fradin, Phys. Rev. B 15, 5119 (1977).

[g] Reference 5.

ies were done on absorbers with Sn concentrations of 1–3 at. %. At such high concentrations, impurity clustering is a possibility which would invalidate the use of a model based on isolated impurities. In Table VII we list the relevant f values which were used in our force-constant ratio calculations (see Table II). For ^{119}Sn in Pd f values and thermal-shift measurements have been analyzed by the authors in terms of impurity moments. These were used by us to recalculate the listed effective host-impurity force-constant ratios in Table II using neutron data for the Pd host moments, instead of Debye spectra as used by the authors. For Sn in Pb the low and the high temperature data are inconsistent (see Table II).

5. *^{197}Au impurity systems*

We have included in Table VII the only known absolute f values of ^{197}Au in Cu and Ag.[5]

C. Effective host-impurity force-constant ratios

In Table II we have collected all effective host-impurity force-constant ratios which could be determined from the f values in columns 6 and 5 of Table VI and VII, respectively, using the method of analysis summarized in Secs. II D 1–II D 3.

In column 4 of Table II we list the quasiharmonic force-constant ratios as obtained from impurity f measurements at temperature T' (column 5) and a host neutron density-of-states function $G(\omega)$ at T_0 (column 6), using Mannheim's integral[4,6] [Eqs. (10a)–(10d), Sec. II D 3]. The values in *italic* print for Cu and Pd represent 0 K extrapolated values (Sec. II D 1). In column 7 we list the force-constant ratios as obtained from low-temperature f measurements ($T' \sim 4$ K) and host moments $\mu(-1)$ from neutron data at T_0 (column 6), using Eq. (15). The values in parentheses are those for which the more appropriate low-temperature host moments from neutron studies were not available. Finally, columns 8 and 9 list the low-temperature force-constant ratios as derived from high and low-temperature f measurements, respectively, and host moments analyzed from heat capacities (see Sec. II D 2).

The following conclusions may be drawn from Table II.

(i) With the exception of ^{57}Fe in Cu or Ni and ^{197}Au in Ag or Cu, all impurity-host interactions are weaker than the host-host interactions ($A/A' > 1$). The 4-K f values for ^{119}Sn in Au and Pb are in doubt.

(ii) The best available data led to the conclusion that in most materials effective host-impurity force-constant ratios deviate from the isotopic impurity value $A/A' \equiv 1$ considerably more than the error range in these ratios.

(iii) Quasiharmonic force-constant ratios from room temperature f data and neutron-host data and low-temperature force-constant ratios from extrapolated $\mu'(-2)$ values and heat-capacity data (Secs. II D 2 and II D 3), listed in columns 4 and 8, are in excellent agreement with each other within their stated precision. In general these values have a higher precision than the corresponding force-constant ratios obtained from low-temperature f values. The reason is that for ^{57}Fe the low-temperature f values are close to unity, thus small errors in f cause large errors in $\ln f$ and $\mu'(-1)$.

(iv) Generally, force-constant ratios calculated from low-temperature f measurements and $\mu(-1)$ values for the hosts agree well between neutron (column 7) and heat-capacity data (column 9). They are also consistent with, though less precise than, the force-constant ratios obtained from near room-temperature f measurements. However, it may be significant that for several of the $3d$, $4d$, and $5d$ transition elements, the low-temperature f values yield systematically higher values of A/A'.

(v) The force-constant ratios of Table II are in a few cases substantially different from those published earlier.[4,11,15,27] This is the result of various changes in impurity and host-data analysis required by the revised internally consistent methodology as presented in this paper. We consider the values listed in Table II the most reliable and physically significant ones obtainable at this time from all published data.

VI. DISCUSSION

A. Force-constant ratios from thermal-shift measurements

As discussed in Sec. II A, thermal-shift (SOD) measurements can, in principle, also be utilized to determine impurity moments, and thus force-constant ratios. This method has two major drawbacks, one theoretical, the other one experimental.

In order to evaluate shift data in terms of the mean-squared velocity $\langle v^2 \rangle$, the chemical [or isomer (IS)] shift must be subtracted. In most such studies, a *temperature-independent* chemical shift has been assumed. Serious doubt about the validity of this assumption has already been cast by the work of Housley and Hess.[33] Even though the temperature dependence of the IS for ^{57}Fe in the metals included in the Housley *et al.* work appears to be small, their data establish only a *lower* limit. Also, it is clear that large differences may occur from one host to another.[33]

The second and more serious problem in the analysis of thermal-shift measurements for the purpose of obtaining reliable effective host-impurity force-constant ratios, in particular for ^{57}Fe im-

purities, is the relative insensitivity of $\langle v^2 \rangle$ to variation in A/A'. We showed in a sample calculation (Ref. 4, Sec. V C) for ^{57}Fe in Pd that a 7% change in A/A' results in a line shift at the most sensitive temperature (0 K) of 0.002 mm/sec, typically an order of magnitude smaller than the errors in published shift data.[32,34]

We suggest, therefore, that accurate shift data could best be used, alternatively, to extend the original work by Housley and Hess[33] with greater reliability in order to determine the temperature dependence of the s-electron density $\langle |\Psi_s(0)|^2 \rangle_T$ by *calculating* the contribution due to SOD from the impurity theory,[6] using the most reliable effective force-constant ratios as determined from precision f measurements.

It has been proposed by Kagan that $f(0\text{ K})$ could be determined *independently* from an integral over the thermal-shift measurements.[35] While in principle this is true, in practice it would require a large number of very accurate shift measurements between 0 and 100 K, where most of the contribution to the integral occurs. Instead, what has been done is to use a functional form to fit the few data points available in order to obtain sufficient precision for the integration. Whether Debye or Mannheim theory is used to generate this curve, the effective force-constant change is implicitly contained in the fitted function. Therefore, no new information is obtained beyond that of fitting the shift data directly. The technique is useful only as a check of internal consistency.[27,36,37]

B. Internal correlation between impurity parameters: McMillan ratio

A series of papers has appeared in the Mössbauer literature[27,36-40] dealing with observed correlations between Mössbauer f values and thermal-shift measurements, and also between impurity and host parameters. In these papers, a key lattice-dynamical quantity investigated is the so-called "McMillan ratio" for the impurity: the ratio of the thermal averages of $[\langle\omega\rangle/\langle\omega^{-1}\rangle]^{\rm imp}$, with

$$\langle\omega^l\rangle^{\rm imp} = \int_0^\infty G'(\omega)[\bar{n}(T)+\tfrac{1}{2}]\omega^l\, d\omega,$$

where $\bar{n}(T)$ is the occupation number (statistical factor).

The fact that the McMillan ratio approaches a constant value at high temperature can be seen by using Eqs. (1a) and (1b) and expanding $\bar{n}(T)$ for high temperatures

$$\left(\frac{\langle\omega\rangle}{\langle\omega^{-1}\rangle}\right)^{\rm imp} = \frac{\frac{1}{3}\langle v^2\rangle_T^{\rm imp}}{\langle x^2\rangle_T^{\rm imp}} = \left[\mu'(-2) + \frac{1}{12}\left(\frac{\hbar}{kT}\right)^2 \times [1-\mu'(2)\mu'(-2)] - \frac{1}{120}\left(\frac{\hbar}{kT}\right)^4 \times \left(\mu'(2) - \frac{1}{6}\mu'(4)\mu'(-2)\right) + \cdots\right]^{-1}. \tag{18}$$

The leading term $1/\mu'(-2)$ shows that this ratio is determined principally by the f data [see Eq. (1a)]. Using typical values for the moments, we find that in most materials the higher-order terms in $1/T$ contribute a correction of no more than a few percent above 150 K. This has also been shown to be true for Fe in Fe.[36,37] The correlation plots of $-\ln f$ versus shift[36,37] emphasize this high-temperature region. Due to the effects of zero-point motion, the variation with temperature of both thermal shift and $-\ln f$ below 150 K is rather small, thus determining only a small portion of the "correlation" (see, e.g., Fig. 3, Ref. 37).

Since in the high-temperature (HT) limit the McMillan ratio of the impurity approaches $1/\mu'(-2)$, we can use the moment expansion from Mannheim theory, Eq. (11), together with Eqs. (3a) and (4) to obtain

$$\left(\frac{\langle\omega\rangle}{\langle\omega^{-1}\rangle}\right)_{\rm HT}^{\rm imp} \to \frac{1}{\mu'(-2)} = \frac{A}{M'}\left(\frac{1}{\beta_{-2}} - 1 + \frac{A}{A'}\right)^{-1}. \tag{19}$$

In the low-temperature (LT) limit, using the approximate expressions Eqs. (15) and (16) and neglecting the small corrections a and b,

$$\left(\frac{\langle\omega\rangle}{\langle\omega^{-1}\rangle}\right)_{\rm LT}^{\rm imp} \to \frac{\mu'(+1)}{\mu'(-1)} \simeq \frac{A}{M'}\left(\frac{A'}{A}\right)^{1/2} \times \beta_{-1}\left(\beta_{+1}\left\{1-\beta_4\left[1-\left(\frac{A}{A'}\right)^{1/2}\right]\right\}\right)^{-1}. \tag{20}$$

Clearly, these two limits are different. For an *isotopic impurity* ($A = A'$), the high- to low-temperature ratio of the limits, Eqs. (19) and (20), is $\beta_{+1}\beta_{-2}/\beta_{-1}$. It has been pointed out[36,37] that the Debye model predicts this ratio of limits to be $\frac{2}{3}$. From the Born–von Kármán calculations for the metals listed in Table I, this ratio differs from the Debye prediction by as much as ±15%. Allowing, in addition, force constants to vary as much as a factor of two, this range of values increases to ±35%. With such a large variance from material to material, the approximation of a constant value of $\frac{2}{3}$ for the ratio of high- to low-temperature limits of $\langle\omega\rangle/\langle\omega^{-1}\rangle$ for the purpose of

obtaining low-temperature lattice parameters from high-temperature measurements is not warranted.[36-39] Conversely, if the low-temperature limit of the McMillan ratio is a desired quantity, it can be obtained most directly from a moment analysis of heat-capacity data, or for an impurity system, from f measurements and Eq. (20).

C. Correlations of impurity to host parameters

1. McMillan ratio with Θ_D

In an extension of the several papers on the McMillan ratio from Mössbauer data, an "unexpected" correlation was reported between the McMillan ratio of the impurity system and properties of the host lattice.[27,38,40] Although the relevant shift data have not been published explicitly, we showed in Sec. VI B that in the high-temperature limit, the McMillan ratio depends, within the accuracy of the experimental data, primarily upon the f values. This follows from the fact that in the classical or near-classical region, the shift depends only upon temperature and not upon properties of the impurity-host system.

Previous papers[38,40] have attempted to correlate the McMillan ratio of the impurity to an effective Debye temperature of the host, suitably modified for mass change: $(M/M')^{1/2}\Theta_D$. The Θ_D used in those studies was that obtained from *low*-temperature heat-capacity measurements $\Theta_D(-3)$. In Fig. 3 we show such a plot, using open circles. The McMillan ratio is given as $1/\mu'(-2)$, where the values have been calculated from the best values of the Mössbauer fraction f (Tables II and VI) at room temperature. The best fit in Refs. 38 and 40 is shown as the broken line.

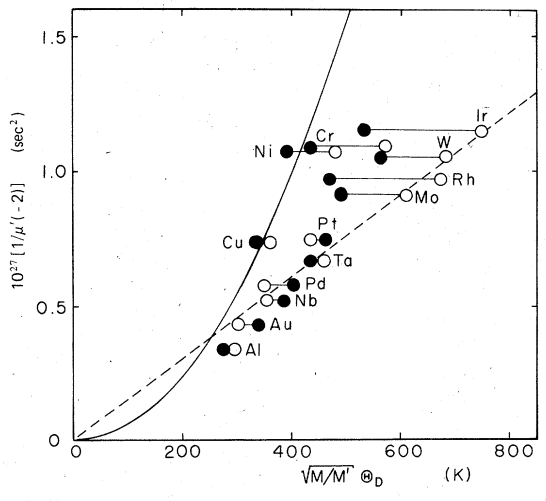

FIG. 3. High-temperature McMillan ratio [Eq. (19)] vs the mass-modified host Debye temperatures: ○, $\Theta_D(-3)$; ●, $\Theta_D(+2)$. The broken line represents the correlation proposed in Ref. 38. The solid line represents the expected relationship for an isotopic impurity, $A = A'$ (see Sec. VI C 1).

Examination of Eq. (19) shows the presence of the factor A/M'. Since $A/M = \mu(+2) = (k/\hbar)^2[\Theta_D(+2)]^2$, it would seem physically more meaningful to use the Debye temperature corresponding to the (+2) moment for the host parameter, since it is directly related to the effective restoring force constant A. $\Theta_D(+2)$ is obtainable from heat-capacity measurements taken in the range 50–150 K by standard techniques (see Sec. IV B).

The solid circles in Fig. 3 indicate the shifts in the points if $\Theta_D(+2)$ is used instead of $\Theta_D(-3)$ for the host. With that choice, $(M/M')^{1/2}\Theta_D(+2) = (A/M')^{1/2}$; we have evaluated the remaining factor in Eq. (19) using the Leighton model value 0.596 for β_{-2} and $A = A'$. This is the solid curve in Fig. 3.

a. Discussion. As we have discussed in the previous Sec. VI C 1, a plot of $[\langle\omega\rangle/\langle\omega^{-1}\rangle]^{\rm imp}_{\rm HT}$ against $(M/M')^{1/2}\Theta_D(-3)$ amounts to a search for a single correlation between the impurity moment $\mu'(-2)$ and a fractional power $(b)^{1/3}$ of the initial curvature of the host density of states function $G(\omega)_{\lim_{\omega\to 0}} = b\omega^2 + \cdots$. Considering the large deviation for at least three well-established data points Cu, Ni, and Cr, we believe that the suggested correlation (dashed line, open circles in Fig. 3) is not well established. If, alternatively, $\Theta_D(+2)$ is chosen for the host parameter, we have from Eq. (19) and Sec. VI C that the resulting scatter of the solid circles relative to the solid curve for $A/A' = 1$ in Fig. 3 is representative of the variations in value of the factor in square brackets of Eq. (19). It contains the force-constant changes A/A' and the variation of the moment ratio β_{-2}. The main conclusion to be drawn from such a plot is a graphical form of that stated in Sec. V C: with the exception of ^{57}Fe in Cu and Ni, most ^{57}Fe-host interactions are *reduced*; $0.8 \lesssim A/A' \lesssim 2.6$.

2. Effective impurity-host force-constant ratio with host force constant

It has also been suggested[27,38] that a correlation might exist between λ'/λ as defined by the strict nearest-neighbor Mannheim model [see Sec. III A and Eq. (10e)] and $C_1^{-1/2}$, a nearest-neighbor *bond-stretching* force constant.[27] Figure 4 shows such a plot of the more meaningful effective impurity-host force-constant ratio A'/A vs $C_1^{-1/2}$ as defined by Chen and Brockhouse.[41] The scatter is similar to that in Fig. 3 with Cu and Ni falling completely outside the suggestive clustering. The absence of a convincing simple correlation also contradicts

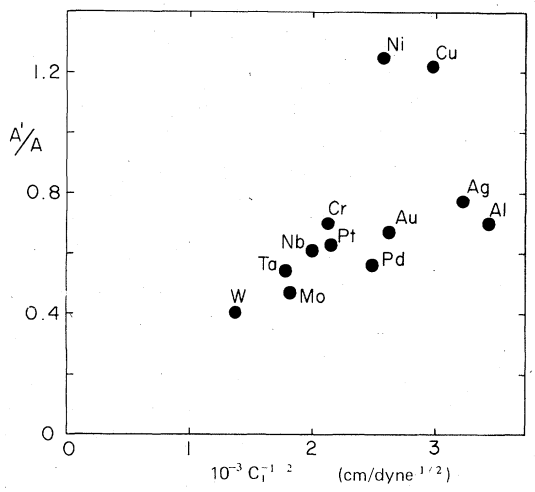

FIG. 4. Effective impurity-host force-constant ratio vs $C_1^{-1/2}$, where C_1 is the nearest-neighbor bond-stretching force constant of the host (see Sec. VI C 2).

the postulated hypothesis that the effective force constant associated with the impurity should be proportional to the geometric mean of the effective force constants for the impurity in bulk and for the host in bulk.[27,38]

3. *A qualitative correlation between impurity lattice dilation and effective impurity-host force-constant ratio for ^{57}Fe impurities*

When Fe is alloyed with various other metals the only two cases known to us where the lattice parameter increases is for the dilute Fe in Cu and Ni alloys. In all other cases the lattice parameter decreases, correlated with $A'/A < 1$.[16] This correlation is not quantitative; a greater lattice contraction is not necessarily correlated with a smaller value of A'/A. On the other hand, for ^{119}Sn or ^{197}Au impurities, the above-mentioned *qualitative* correlation between effective force-constant ratio and lattice dilation does not seem to hold.

4. *Conclusion*

In light of the fact that no single-host parameter has been found that correlates unambiguously with the observed trends in effective force-constant ratios, we conclude that these changes must depend upon a yet unknown combination of several parameters.

VII. SUMMARY AND CONCLUSION

We have critically reviewed the various simplified models which have been used to extract effective host-impurity force-constant ratios from Mössbauer fraction and thermal-shift measurements. We have shown that unnecessary systematic errors are introduced by oversimplified impurity models or by the use of inappropriately matched data for the pure host materials. These systematic errors tend to deceptively compress the range of resulting force-constant changes. This has led in the past to the conclusion that metal impurities in pure-metal hosts behave like isotopic impurities. Although it is true that the range of mass changes in the systems studied so far is larger ($0.3 < M'/M < 3.5$) than that of the effective force-constant changes ($0.65 < A/A' < 2.6$), the deviations from the isotopic impurity value $A/A' \equiv 1$ are in most cases significantly larger than the uncertainties in these ratios.

We found remarkable uniformity within the groups of fcc and bcc metals in the values of certain moment ratios. Also, there is generally good agreement between moments derived from neutron-dispersion measurements and those from an analysis of heat-capacity data.

Using the restrictive assumptions of Mannheim's analytical impurity theory for cubic metals, we have derived analytical relations between even impurity to host-moment ratios, mass ratio, and force-constant ratio. From a numerical analysis we were also able to find approximate relations for some experimentally important odd-moment ratios. These expressions for the moment ratios, which can be obtained from Mössbauer impurity and neutron or heat-capacity host data, can be conveniently applied to obtain reliable effective host-impurity force-constant ratios by an internally consistent method of analysis.

We conclude that, in contrast with earlier suggestions, these force-constant ratios cannot be simply correlated with any one parameter which characterizes the particular impurity-host system. Until the time that band theory may be able to handle predictions of force constants in metals, this set of best presently available effective host-impurity force-constant ratios will have to stand by itself. Improvements in the reliability of such data could come from additional *low-temperature* neutron-dispersion studies in several host metals in which anharmonic effects presently contribute to uncertainties in the physical interpretation of such force-constant ratios, as well as from additional precision Mössbauer studies to remove certain inconsistencies in the impurity data.

ACKNOWLEDGMENTS

We like to thank Dr. J. S. Semura for helpful discussions of some of the theoretical problems related to this work and we are grateful to Dr. R. D. Taylor and Dr. D. J. Erickson for their communication of some unpublished data. The meticulous work of Ms. V. Pfaff was very much ap-

preciated.

APPENDIX: MOMENTS OF THE DYNAMIC RESPONSE FUNCTION AT THE IMPURITY SITE

The equations of motion of an atom in the direction $\alpha(=x, y, z)$ at site l (one atom per unit cell) in a harmonic crystal is given by

$$M(l)\ddot{u}_\alpha(l,t)+\sum_{\beta,l'}A_{\alpha\beta}(l,l')u_\beta(l',t)=0, \tag{A1}$$

where $M(l)$ is the atomic mass at l and $u_\alpha(l,t)$ is its displacement. $A_{\alpha\beta}(l,l')$ stands for the $\alpha\beta$ component of the force constant between atoms at l and l'. When the mass differs from site to site it is more convenient to introduce the dynamical matrix

$$D_{\alpha\beta}(l,l')=A_{\alpha\beta}(l,l')/[M(l)M(l')]^{-1/2}. \tag{A2}$$

Then, assuming a harmonic vibration of frequency ω, Eq. (A1) is reduced to

$$\sum_{\beta,l'}[M(l)]^{1/2}[D_{\alpha\beta}(l,l')-\omega^2\delta_{\alpha\beta}\delta(l,l')][M(l')]^{1/2}u_\beta(l')=0, \tag{A3}$$

or, in matrix form

$$\underline{L}(\omega^2)\underline{U}=0, \tag{A4}$$

where $\underline{L}(\omega^2)$ is the lattice matrix

$$\underline{L}(\omega^2)=\underline{M}^{1/2}(\underline{D}-\omega^2\underline{I})\underline{M}^{1/2}. \tag{A5}$$

Note that in Eq. (A5) the sign is different from that used customarily, but the same as that introduced by Mannheim and Cohen.[6]

The inverse of the lattice matrix is the Green's function

$$\mathcal{G}_{\alpha\beta}(l,l';\omega^2)=\frac{1}{[M(l)M(l')]^{-1/2}}\sum_s\frac{T^{*s}_\alpha(l)T^s_\beta(l')}{\omega_s^2-\omega^2}, \tag{A6}$$

where $T^s_\alpha(l)$ is an element of a unitary matrix which diagonalizes the dynamical matrix

$$\sum_{\alpha\beta ll'}T^s_\alpha(l)D_{\alpha\beta}(l,l')T^{*s'}(l')=\omega_s^2\delta_{ss'}. \tag{A7}$$

The unitary matrix has the following properties

$$\sum_{\alpha,l}T^{*s}_\alpha(l)T^{s'}_\alpha(l)=\delta_{ss'},$$

and

$$\sum_s T^{*s}_\alpha(l)T^s_\beta(l')=\delta_{\alpha\beta}\delta(l,l'). \tag{A8}$$

We note that $\mathcal{G}_{\alpha\alpha}(0,0;\omega^2)$ is a generating function of moments of the density of states at the lattice coordinate origin. Since

$$\mathcal{G}_{\alpha\alpha}(0,0;\omega^2)=\frac{1}{M(0)}\sum_s\frac{T^{*s}_\alpha(0)T^s_\alpha(0)}{\omega_s^2-\omega^2}, \tag{A9}$$

by expanding this expression in the power series of ω^{-2} for large ω^2 $[\omega^2>\max\{\omega_s^2\}]$, we have

$$\mathcal{G}_{\alpha\alpha}(0,0;\omega^2)=-\frac{1}{M(0)\omega^2}\sum_n\sum_s|T^s_\alpha(0)|^2(\omega_s/\omega)^{2n}. \tag{A10}$$

If we define the nth *site moment* of the density of states by

$$\mu_\alpha(l;n)=\sum_s^\infty|T^s_\alpha(l)|^2\omega_s^n, \tag{A11}$$

then Eq. (A10) leads to

$$\mathcal{G}_{\alpha\alpha}(0,0;\omega^2)=-\frac{1}{M(0)\omega^2}\sum_{n=0}\frac{1}{\omega^{2n}}\mu_\alpha(0;2n). \tag{A12}$$

On the other hand, if we can assume that the lattice is of a finite size, so that we can choose the value of ω^2 in Eq. (A9) smaller than any ω_s^2, we have

$$\mathcal{G}_{\alpha\alpha}(0,0;\omega^2=0)=[1/M(0)]\mu_\alpha(0;-2). \tag{A13}$$

For a perfect crystal, the normal mode s can be represented by the branch index j and the wave vector $\vec{k}$ because of the translational and reflection symmetry. Then, the transformation matrix $T^s_\alpha(l)$ can be replaced by $\sigma^j_\alpha(\vec{k})\exp[i\vec{k}\cdot\vec{R}(l)]/\sqrt{N}$, where $\sigma^j_\alpha(\vec{k})$ is the eigenvector of the dynamical matrix belonging to the normal mode $(j\vec{k})$ and N is the number of atoms in the lattice. For a perfect cubic lattice, $|T^s_\alpha(l)|^2=|\sigma^j_\alpha(k)|^2/N=1/3N$, so that the above definition of moments, Eq. (A11), reduces to the usual expression, Eq. (2a), Sec. II B, i.e., $\mu_\alpha(l;n)_{\text{cubic}}=(1/3N)\sum_s\omega_s^n$.

The change of the lattice Green's function due to a substitutional impurity at the origin has been calculated for a fcc and a bcc lattice, assuming nearest-neighbor central forces, by Mannheim,[6] and for a simple cubic lattice (Visscher[9]) by Ohashi and Kobayashi.[11] After a slight modification, those results can be expressed in the same following form:

$$\mathcal{G}'_{\alpha\alpha}(0,0;\omega^2)=\frac{M-(\lambda/A)+[1-\lambda(M/A)\omega^2]\mathcal{G}_{\alpha\alpha}(0,0;\omega^2)}{M'\quad 1+\rho(\omega)[1+M\omega^2\mathcal{G}_{\alpha\alpha}(0,0;\omega^2)]}, \tag{A14}$$

where the impurity atom is at $l=0$. Primed quantities refer to the impure lattice or the impurity atom and $\lambda=1-A_{xx}(0,0)/A'_{xx}(0,0)$ and $A=A_{xx}(0,0)$ [see Eqs. (3b) and (3c)]. The function $\rho(\omega)$ is given by Eq. (10b). It is interesting to note that Eq. (A14) can be easily shown to hold also for a linear chain.

Expanding the right-hand side of Eq. (14) for large values of ω^2 and using Eq. (A12), the impurity Green's function can be expressed in terms

of the *even* moments

$$\mathcal{G}'_{\alpha\alpha}(0,0;\omega^2) = -\frac{1}{M'\omega^2}\left[1+\frac{M}{M'\omega^2}\frac{\mu(2)}{1-\lambda(M/A)\mu(2)} + \frac{M}{M'\omega^4}\left(\frac{\mu(4)}{1-\lambda(M/A)\mu(2)} + \frac{[(M/M')-1]\mu^2(2)+\lambda(M/A)\mu(2)\mu(4)}{[1-\lambda(M/A)\mu(2)]^2}+\cdots\right)\cdots\right]. \quad \text{(A15)}$$

Here, the moments appearing on the right-hand side are for the pure lattice. They do not depend on the site nor on the direction, so that the symbols α and l are suppressed. The left-hand side of Eq. (A15) can be expanded in terms of $\mu'_\alpha(0;2n)$ by using Eq. (A12) for the impure lattice. Again, the subscript α can be suppressed. Comparing the coefficients of the power series in ω^{-2n} on both sides, we can easily find the change in even moments at the impurity site. Defining as in Eq. (4),

$$\beta_n = \frac{1}{\mu(n)}\left(\frac{A}{M}\right)^{n/2} = [\mu(n)]^{-1}[\mu(2)]^{n/2} \quad \text{(A16)}$$

for the pure lattice and noting that $\beta_2 = 1$, we find

$$\frac{\mu'(0;2)}{\mu(2)} = \left(\frac{M}{M'}\right)\left(\frac{A'}{A}\right), \quad \text{(A17)}$$

identical with the result of the Einstein model, Eq. (6) for $n=2$. However, for $n=4$ we find

$$\frac{\mu'(0;4)}{\mu(4)} = \left(\frac{M}{M'}\right)\left(\frac{A'}{A}\right)^2\left[1-\beta_4\left(1-\frac{M}{M'}\right)\right], \quad \text{(A18)}$$

and putting $\omega^2 = 0$ in Eq. (A14), using the definition Eq. (A13),

$$\frac{\mu'(0;-2)}{\mu(-2)} = \left(\frac{M'}{M}\right)\left[1-\beta_{-2}\left(1-\frac{A}{A'}\right)\right]. \quad \text{(A19)}$$

β_4 and β_2 are empirically found to have values of about 0.8 and 0.6, respectively (see Table I).

It should be noted that the above relations include the contributions of localized modes where present (see Sec. III A).

We attempted to derive similar functional relationships for odd impurity site moments which are important for the analysis of Mössbauer data at low temperatures. These attempts were not successful (see, however, Sec. III B).

*Research supported by NSF Research Grant No. DMR74-14438 and Portland State University.

†Present address: New Jersey Institute of Technology, Newark, N. J. 07102.

[1]J. Bara and A. Z. Hrynkiewicz, Phys. Status Solidi 15, 205 (1966).

[2]S. M. Qaim, J. Phys. F 1, 320 (1971).

[3]V. A. Bryukhanov, N. N. Delyagin, and Yu. Kagan, Sov. Phys.-JETP 19, 563 (1964); V. A. Bryukhanov, N. N. Delyagin, and V. S. Shpinel', *ibid.* 20, 55 (1965).

[4]D. G. Howard and R. H. Nussbaum, Phys. Rev. B 9, 794 (1974), especially "Note added in proof."

[5]J. F. Prince, L. D. Roberts, and D. J. Erickson, Phys. Rev. B 13, 24 (1976).

[6]P. D. Mannheim, Phys. Rev. 165, 1011 (1968); P. D. Mannheim and S. S. Cohen, Phys. Rev. B 4, 3748 (1971); and P. D. Mannheim, *ibid.* 5, 745 (1972).

[7]R. M. Housley and F. Hess, Phys. Rev. 146, 517 (1966).

[8]S. S. Cohen, R. H. Nussbaum, and D. G. Howard, Phys. Rev. B 12, 4095 (1975).

[9]W. M. Visscher, Phys. Rev. 129, 28 (1963).

[10]A. A. Maradudin and P. A. Flinn, Phys. Rev. 126, 2059 (1962).

[11]K. Ohashi and K. Kobayashi, J. Phys. F 5, 1466 (1975).

[12]The quantities $A_{\text{eff}}(T)$ and $A'_{\text{eff}}(T)$ were defined in Eqs. (4a) and (4b) and Fig. 1 of Ref. 8.

[13]For example, T. H. K. Barron, W. T. Berg, and J. A. Morrison, Proc. R. Soc. Lond. A 242, 478 (1957).

[14]A. A. Maradudin, P. A. Flinn, and S. Ruby [Phys. Rev. 126, 9 (1962), part V] derive an analytical expression for $\mu'(+2)/\mu(+2)$. However, their $\mu'(+2)$ represents an average moment for the impure lattice, rather than the impurity site moment as in our equation (11).

[15]W. A. Steyert and R. D. Taylor, Phys. Rev. 134, A716 (1964).

[16]R. H. Nussbaum, D. G. Howard, W. L. Nees, and C. F. Steen, Phys. Rev. 173, 653 (1968).

[17]A. P. Miiller and B. N. Brockhouse, Can. J. Phys. 49, 704 (1971).

[18]H. J. Lipkin, Ann. Phys. (N.Y.) 23, 28 (1963).

[19]P. G. Dawber and R. J. Elliott, Proc. R. Soc. Lond. A 273, 222 (1963).

[20]J. L. Feldman and G. K. Horton, Phys. Rev. 137, A1106 (1965).

[21]Y. S. Touloukian and E. H. Buyco, *Thermophysical Properties of Metals* (Plenum, New York, 1970), Vol. 4.

[22]N. E. Phillips, *CRC Critical Reviews in Solid State Science* (Chemical Rubber, Cleveland, 1971), Vol. 2, p. 467.

[23]G. T. Furukawa, M. L. Reilly, and J. S. Gallagher, J. Phys. Chem. Ref. Data 3, 197 (1974).

[24]A. Konti, J. Chem. Phys. 55, 3997 (1971).

[25]L. S. Salter, Adv. Phys. 14, 1 (1965).

[26]R. Colella and B. W. Batterman, Phys. Rev. B 1, 3913 (1970).

[27]R. D. Taylor, D. J. Erickson, and T. A. Kitchens, J. Phys. (Paris) Suppl. 37, C6-35 (1976).

[28]J. J. Bara, *Proceedings of the Conference on Application of the Mössbauer Effect, Tihany, 1969*, edited by

I. Dezsi (Akademiai Kiado, Budapest, 1971), p. 93.
[29]*Mössbauer Effect Data Index*, edited by J. G. Stevens and V. E. Stevens (IFI-Plenum, New York, 1966).
[30]C. F. Steen, D. G. Howard, and R. H. Nussbaum, Solid State Commun. 10, (E)584(a) (1972).
[31]D. G. Howard, R. H. Nussbaum, C. F. Steen, and A. Venkatachar, Bull. Am. Phys. Soc. 16, 835 (1971).
[32]A. Simopoulos and I. Pelah, J. Chem. Phys. 51, 5691 (1969); K. Mahesh, Phys. Status Solidi B 61, 695 (1974).
[33]R. M. Housley and F. Hess, Phys. Rev. 164, 340 (1967).
[34]T. A. Kitchens, W. A. Steyert, and R. D. Taylor, Phys. Rev. 138, A467 (1965).
[35]Yu. Kagan, Sov. Phys.-JETP 20, 243 (1965).
[36]R. D. Taylor and P. P. Craig, Phys. Rev. 175, 782 (1968).
[37]T. A. Kitchens, P. P. Craig, and R. D. Taylor, *Mössbauer Effect Methodology*, edited by I. J. Gruverman (Plenum, New York, 1969), Vol. 5, p. 123.
[38]P. P. Craig, T. A. Kitchens, R. D. Taylor, and J. C. Norvell, Phys. Rev. Lett. 25, 1195 (1970).
[39]P. P. Craig, T. A. Kitchens, and R. D. Taylor, Phys. Rev. B 1, 1103 (1970).
[40]R. D. Taylor, J. C. Norvell, and T. A. Kitchens, *Proceedings of the Twelfth International Conference on Low Temperature Physics*, edited by E. Kanda (Kyoto, 1970), p. 285.
[41]S. H. Chen and B. N. Brockhouse, Solid State Commun. 2, 73 (1964).